國立臺灣大學生命科學院生態學與演化生物學研究所

博士論文

Institute of Ecology and Evolutionary Biology

College of Life Science

National Taiwan University

Doctoral Dissertation

晚熟鳥錦花雀與早熟鳥雞在初生絨毛發育上基因調控之差異

Regulatory Differences in Natal Down Development between

Altricial Zebra Finch and Precocial Chicken

陳志冠

Chih-Kuan Chen

指導教授：丁照棣 & 李文雄

Advisor: Chau-Ti Ting & Wen-Hsiung Li

中華民國 106 年 1 月

January 2017

謝辭

終於走到博士生生涯的尾聲了。

　　回想這段長久的日子，無論是過程或結果，無論是人或事物，都是當初料想不到的。曾經聽信謠言，以為只要拿到學位，人生就此一帆風順，卻直到現在才發現，博士根本就滿街跑。幸運的是在李文雄以及丁照棣老師底下學習，有機會看到不同的世界，了解到甚麼是真正的科學，甚麼是做事該有的態度，也因而漸漸了解自己能做甚麼、該做甚麼。這些意外的經歷，打磨了過去天真的我，而成就了現在的我。

　　在一個大實驗室待很久，又有眾多合作對象，要感謝的人實在寫不完，就感謝整個實驗室吧。感謝李文雄老師實驗室的成員們，有你們當夥伴，讓我每天都充滿動力。感謝丁照棣老師實驗室的成員們，一起讀書開會的日子，讓我增廣見聞。感謝鄭旭辰老師實驗室的成員們，讓我熬過了冗長的動物實驗。也感謝鍾正明老師、吳平老師、呂美曄學姐、李松洲學長的大力協助，研究才得以完成。最後要特別要感謝黃貞祥學長，多年來從學長身上學到的，不是甚麼實驗技術，而是態度。

　　實驗室之外，要感謝的人就更多了。雖然家人朋友們應該永遠也搞不懂我花了這麼多時間是在做甚麼？對社會能有甚麼貢獻？但是你們無差別的耐心支持以及陪伴，是我一路苦撐的主要支柱。尤其感謝爸媽跟老弟，陪伴我走過一次次的低潮；感謝我的老婆，永遠的相信與支持。我想最好的報答大家的方式，就是讓自己坐在最適合的位置，對身邊的人以及社會做出更大的貢獻，所以感謝就到邊，而人生，才開始要踩出去而已。

ABSTRACT (Chinese)

　　鳥類可以分成晚熟與早熟鳥兩個大群，晚熟鳥的幼雛通常絨毛稀疏而皮膚裸露，早熟鳥則通常全身覆蓋著絨毛。一般認為，這種形態上的差異是跟環境的適應有關，但是背後的分子機制仍然不明朗。在本研究中，我以晚熟的錦花雀以及早熟的雞作為研究的模式物種。錦花雀的幼雛具有皮膚裸露的前背部，以及部份長有絨毛的後背部。藉由高通量的轉錄組定序與分析，我比較了前背部與後背部的基因表現，結果發現促進羽毛生長相關的基因 *SHH* (sonic hedgehog)在後背部有較高的表現量。此外，資料分析也顯示 FGF/MAPK 訊息路徑可能跟前背部絨毛的生長抑制相關，而 FGF16 (fibroblast growth factor 16)可能是這個訊息路徑的上游調控因子。將 *FGF16* 以病毒表現系統異位表現於雞胚胎的腿部，結果該部位的絨毛生長被抑制，出現類似錦花雀胚胎前背部的樣式，而且該部位 *SHH* 的表現量減少，又一個已知的羽毛抑制因子 *FGF10* 的表現量則增加。因此，我認為 FGF16 相關的分子訊息抑制了絨毛的生長，進而造成了錦花雀幼雛裸露的前背部。本研究闡述了早晚熟鳥之間絨毛生成可能的基因調控差異。

關鍵字: 早熟鳥；晚熟鳥；羽毛演化；絨羽；錦花雀

ABSTRACT (English)

Birds can be classified into altricial and precocial. The hatchlings of altricial birds are almost naked, whereas those of precocial birds are covered with natal down. This regulatory divergence is thought to reflect environmental adaptation, but the molecular basis of the divergence is unclear. To address this issue, I chose the altricial zebra finch and the precocial chicken as the model animals. Anatomical analysis revealed that zebra finch hatchlings showed suppressed natal down growth in anterior dorsal (AD) skin but partially down-covered posterior dorsal (PD) skin. A comparison of the transcriptomes of AD and PD skins revealed a higher expression level of the feather growth promoter *SHH* (sonic hedgehog) in PD skin than in AD skin. Moreover, the data suggested that the FGF/MAPK signaling pathway is involved in natal down growth suppression and that FGF16 (fibroblast growth factor 16) is an upstream signaling suppressor. Ectopic expression of *FGF16* on chicken leg skin showed downregulation of *SHH*, upregulation of the feather growth suppressor *FGF10*, and suppression of feather bud elongation, similar to the phenotype found in zebra finch embryonic AD skin. Therefore, I propose that FGF16 related signals suppress natal down elongation and cause the naked AD skin in zebra finch. This study provides insights into the regulatory divergence in natal down formation between precocial and altricial birds.
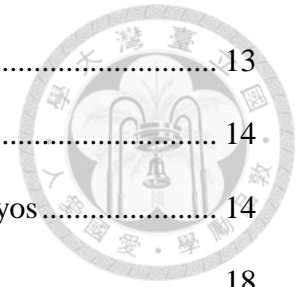
Key words: altricial bird; precocial bird; feather evolution; natal down; zebra finch

OUTLINE

LIST OF FIGURES

vi

LIST OF TABLES

1 Introduction

1.1 Background and significance

Modern birds are highly diverse with more than 10,000 species and represent the most abundant vertebrate lineage (Wright 2006). They possess many evolutionary innovations, such as feathers, toothless beaked jaws, the laying of hard-shelled eggs, a high metabolic rate, and a lightweight but strong skeleton, enabling them to occupy different environmental niches. Birds provide an excellent model to study animal evolution and environmental adaptations.

1.1.1 Feather diversity and bird diversity

Among the evolutionary novelties in birds, the feathers show the highest degree of complexity and diversity (Prum and Brush 2002; Prum 2005; Chen, et al. 2015; Strasser, et al. 2015). Feather diversity offers diverse functions to a bird. For example, contour feathers form the outline of the body and provide physical protection, tail feather maintain the body balance, flight feathers enable the bird fly, down feathers keep the body worm, semiplume feathers are used for insulation, and bristle feathers are specialized feathers that may have a tactile function (Podulka, et al. 2004) (Figure 1). Feather diversity offers different survival advantages to different birds; for example, colorful feathers can be used to send visual signals within species. Feather is an excellent model for studying how animals adapt to different environments, studying how feather diversity contributes to avian diversity is my major interest.

1
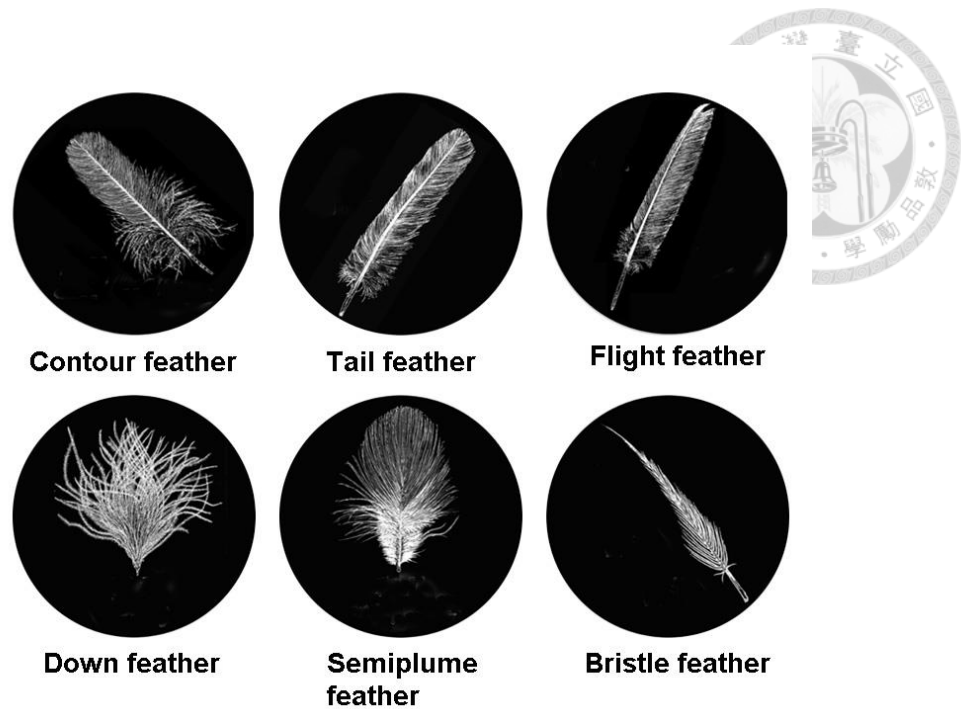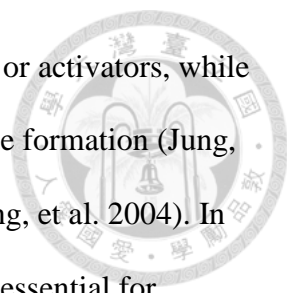
Figure 1. Types of bird feathers. (Illustrated by Siao-Man Wu).

1.1.2 Feather development and the molecular mechanisms

Feather distributions in avian skin have two spatial patterns: in the macropattern the feather tracts are separated by bare skin, while the micropattern shows regular spacing between individual feathers (Olivera-Martinez, et al. 2004; Mou, et al. 2011). The periodic skin micropatterning is achieved by the action of opposing feather growth activators and inhibitors to form a reaction diffusion mechanism (Meinhardt and Gierer 2000; Mou, et al. 2011). The epithelio-mesenchymal molecular interactions between the dermis and the overlying epidermis coordinate the spatial arrangement and regular outgrowth of feathers (Hornik, et al. 2005; Mou, et al. 2011; Wells, et al. 2012).

Many molecules that regulate feather formation have been identified. For example, WNT/β-catenin signaling and cDermal-1 are promoters at the early stages of skin patterning (Noramly, et al. 1999; Widelitz, et al. 2000; Hornik, et al. 2005). Some FGFs

2

(fibroblast growth factors) and SHH (sonic hedgehog) are promoters or activators, while BMPs (bone morphogenetic proteins) are inhibitors in feather placode formation (Jung, et al. 1998; Mandler and Neubuser 2004; McKinnell, et al. 2004; Song, et al. 2004). In contour feathers, the interactions between α- and β-keratin genes are essential for feather formation and for the morphological and structural diversity of different feather types (Ng, et al. 2015; Bhattacharjee, et al. 2016). Furthermore, the genes underlying some partial or complete featherless mutants have also been characterized in chicken (*Gallus gallus*). The regulatory differences in BMPs cause the naked neck phenotype in chicken, and a nonsense mutation in FGF20 is associated with the featherless trait (Mou, et al. 2011; Wells, et al. 2012).

However, despite the large number of studies in feather development in past decades, the molecular mechanisms responsible for feather diversity and environmental adaptation were not well understood. How the molecular regulatory changes contributed to feather diversity among birds is the specific question I want to ask.

1.1.3 Altricial and precocial birds

Altricial and precocial birds were chosen as the model to study feather diversity. Avian hatchlings display variation in maturity. The hatchlings of altricial birds, such as parrots and songbirds, are close to the embryonic state. In contrast, precocial hatchlings, such as chicken and duck, are close to the adult state (Vleck and Vleck 1987; Starck and Ricklefs 1998). The divergence of altricial and precocial birds might have evolved from habitat selection. The altricial birds tend to nest above grounds, and their chicks need to spend more time on the nest until they can leave the nest on their own (Bicudo 2010). In contrast, the precocial birds tend to be ground nesting, and their chicks can walk away from the nest soon after hatching.

3

I chose altricial and precocial birds as the model to study feather diversity for several reasons. First, feather diversity is important to altricial and precocial bird divergence. The precocial to altricial continuum (or spectrum) has been characterized previously (Starck and Ricklefs 1998) and is briefly summarized below (Table 1). Natal down is the down feather of the hatchlings. The natal down plumage is one of the criteria and is the only discrete indicator to distinguish altricial birds form precocial birds. The hatchlings of altricial birds are almost naked but those of precocial birds are covered with natal down. Second, different survival advantages are found between altricial and precocial birds, suggesting that the altricial and precocial bird divergence associates with bird diversity. Compared to precocial hatchlings, altricial hatchlings show no thermogenic capacity, less locomotor ability, and less growth after fledging, but show larger increases in brain function in postnatal growth (Starck and Ricklefs 1998; Charvet and Striedter 2011). In adults, compared to precocial birds, altricial birds tend to have more complex nests, nest at higher places, invest more offspring care and have better vocal learning ability (Starck and Ricklefs 1998; Bicudo 2010). Third, precocial birds are thought to be the ancestral form of birds on the basis of phylogenetic analysis (Figure 2A) (Starck and Ricklefs 1998; Charvet and Striedter 2011), and the recent fossil record (Figure 2B) (Zhou and Zhang 2004). The early evolved precocial birds may occupy the ground and the later evolved altricial birds were forced to seek for higher habitats. To sum up, altricial and precocial bird divergence was associated with feather diversity and contributes to avian diversity. Therefore, altricial and precocial birds were chosen as the model to study feather diversity in this dissertation.

A
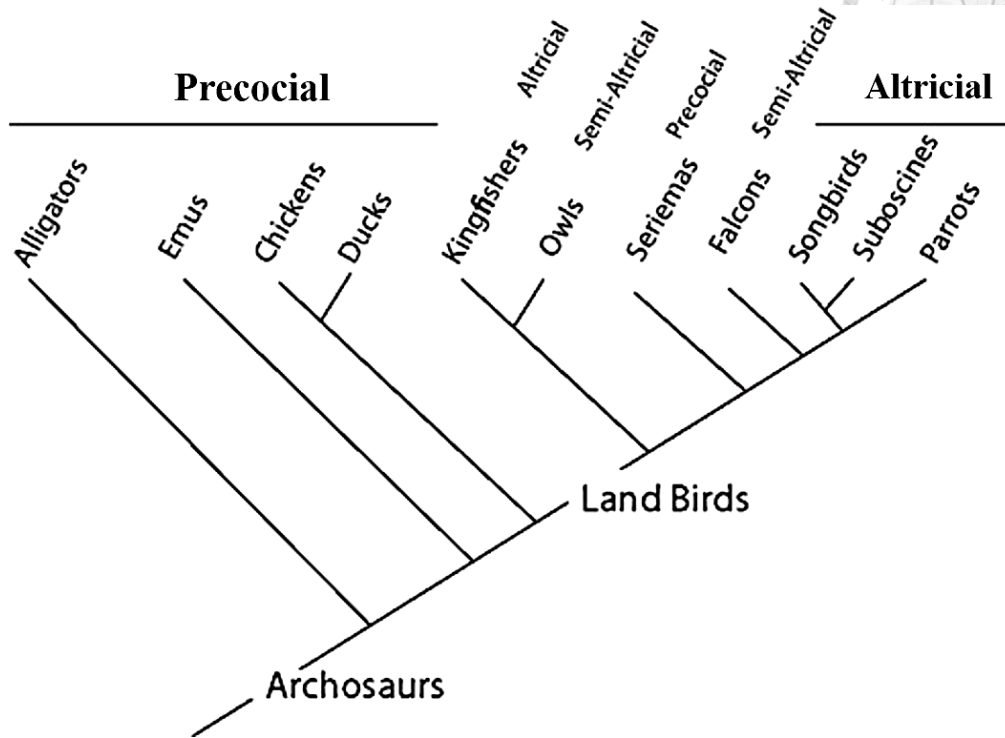
B
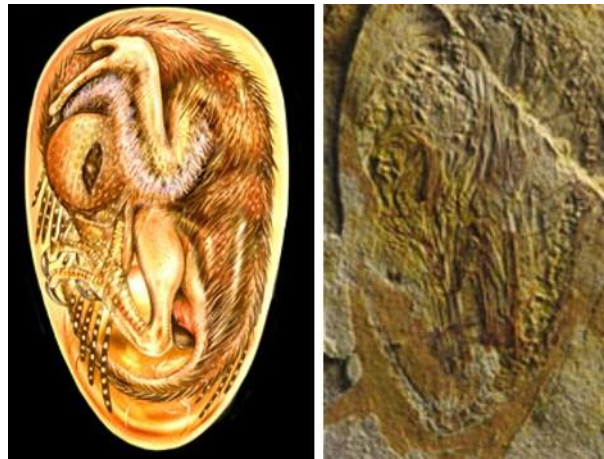
Figure 2. The evolution of altricial and precocial birds. (A) The evolution of altricial and precocial birds based on the phylogeny. Modified from a previous study (Charvet and Striedter 2011). (B) The most intact bird embryo fossil is covered with down feather (adopted from Zhou and Zhang 2004).

5
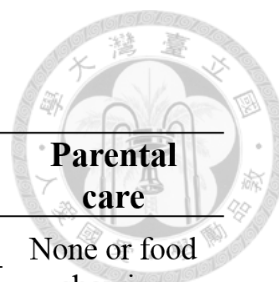
Table 1. The criteria of the precocial to altricial continuum.

DM	Plumage	Eyes	Nest attendance	Parental care
Precocial			Leave	None or food showing
Semiprecocial	Contour feathers or natal down	Open	Nest area	
Semialtricial			Stay	Parental feeding
Altricial	Few or none	Closed		

Note: modified from previous study (Starck and Ricklefs 1998); DM: developmental mode.

1.1.4 Zebra finch and chicken as the altricial and the precocial model

To address the above question, the altricial zebra finch (*Taeniopygia guttata*) and the precocial chicken (*Gallus gallus*) were chosen as the model animals. Zebra finch and chicken are two species with a high quality genome sequence and good annotation (Consortium 2004; Alev, et al. 2009; Greenwold and Sawyer 2010; Warren, et al. 2010). They diverged about 70 to 100 million years ago, which is close to the avian radiation (Warren, et al. 2010). Zebra finch is an important model animal for neuroscience, behavior genetics, comparative physiology as well as ecology (Zann 1996; Adkins-Regan 2009; Clayton, Balakrishnan, et al. 2009; Clayton, George, et al. 2009; Pinaud 2010). Chickens have been studied in population genetics, cell biology, developmental biology, poultry and anatomy (Hamburger and Hamilton 1992a; Brown, et al. 2003; Sang 2004; Stern 2004, 2005). In addition, it is the only bird could be genetically manipulated (Sang 2004). The domestic chicken has many strains. I used White leghorn chicken in this study because it is the most commonly used chicken

6

strain in experiments and its white feather could avoid the experimental influence from the pigments.
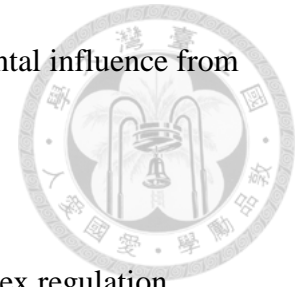
1.2   Specific aims and experimental design

Feather development involves numerous molecules and complex regulation, making it difficult to find the key regulators. Next generation sequencing technologies have revolutionized the study of functional genomics (McDevitt and Rosenberg 2001; Metzker 2005; Mardis 2008b, a; Schuster 2008). I took advantage of the power of RNA-seq to compare the transcriptomes of different skin regions and different developmental stages to identify candidate regulators.

To investigate regulatory differences in natal down development between altricial zebra finch and precocial chicken, I pursued the following aims:

Aim1: Characterizing the developmental states of feather on embryos and hatchlings of zebra finches and chickens.

I collected zebra finch and chicken embryos at different embryonic incubation days (Figure 3). By observing their developments, I defined the feather formation types in skin regions with or without natal down growths in zebra finch and chicken. I further utilized paraffin sections with H&E (hematoxylin and eosin) stain and immunohistochemical stains to characterize the cellular level differences in different types of feather formation.

Aim2: Characterizing the molecular changes underlying the natal down growth divergence.

I used comparative transcriptomics to identify the molecular changes between different types of feather formation in zebra finch. To identify the gene regulatory pathways responsible for feather growth divergence, I selected the candidate genes by

7

clustering analysis, differentially expressed gene (DEG) analysis, and gene pathway enrichment.
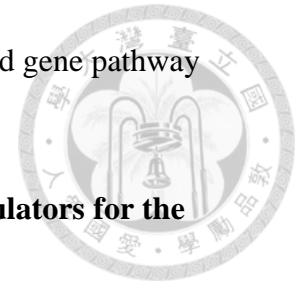
Aim3: Identifying and functionally validating the candidate regulators for the natal plumage growth divergence.

To functionally validate the causative regulators for feather growth divergent, I used the RCAS (replication-competent ASLV long terminal repeat with a splice acceptor) virus system to overexpress the candidate genes in chicken (Hughes 2004). The results were confirmed by analyzing the expression of the downstream genes and by immunohistochemical stains.
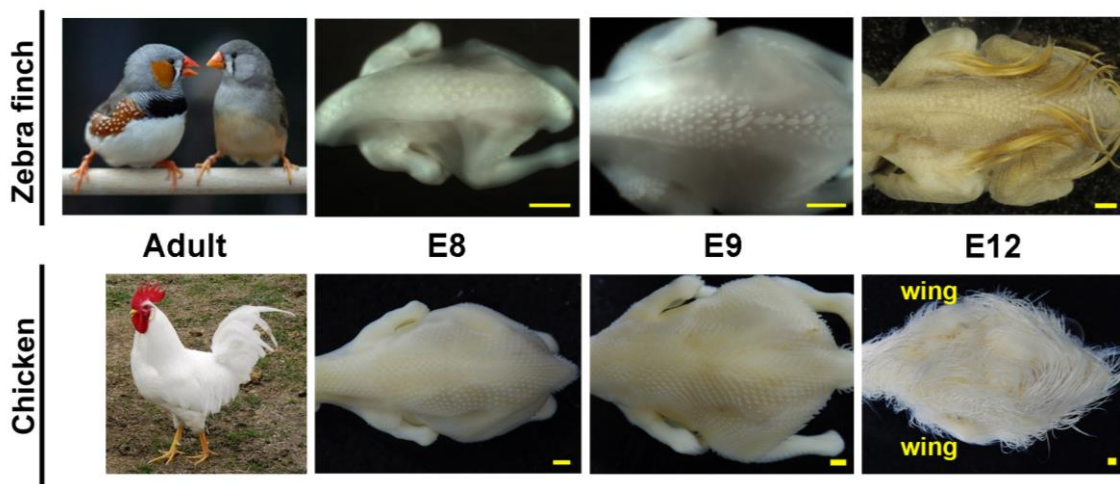
Figure 3. Adults and embryonic developments of altricial zebra finch and precocial chicken. E8, E9, and E12: embryonic incubation days 8, 9, and 12. Scale bar: 0.1 cm.

2 Materials and Methods

2.1 Ethics statement

All the animal experiments in this study were conducted according to the protocol approved by the Institutional Animal Care and Use Committees of National Chung Hsing University (Taichung, Taiwan).

2.2 Eggs and animals

Pairs of adult zebra finches were purchased from a breeder in Tainan, Taiwan, and their fertilized eggs were collected for the study. The white leghorn chicken was used as the precocial bird model to avoid blocking the signal from *in situ* hybridization by feather pigmentation. The pathogen free fertilized chicken eggs were obtained from the farm of National Chung Hsing University. All of the eggs used were incubated at 38℃ and in relative humidity 65% until the specific stages. The stages and corresponding incubation days of zebra finch embryos followed the description of Murray et al. (Murray, et al. 2013), and the stages and corresponding incubation days of chicken embryos followed the description of Hamburger and Hamilton (Hamburger and Hamilton 1992b). For example, E8 means embryonic incubation days 8, E12 means embryonic incubation days 12, and D1 means posthatch day 1. The corresponding stages between chicken and zebra finch embryos followed the supplementary description of Abzhanov et al. (Abzhanov, et al. 2004). The chicken and zebra finch showed similar development within E12.

2.3 Paraffin section and immunohistochemistry

The chicken and zebra finch embryos were fixed in 4% paraformaldehyde at 4℃ overnight. Paraffin sections of 5 μm were conducted following the procedure of Chuong et al. (Chuong 1998). For immunohistochemical staining, PCNA (proliferating cell

9

nuclear antigen) antibody was purchased from Chemicon (CBL407), AMV-3C2 (Gag-pro antibody) antibody was from Developmental Studies Hybridoma Bank, and CDH1 (E-cadherin) antibody was from BD Biosciences (610182). DAPI (4',6-diamidino-2-phenylindole) was used to visualize the nuclei.
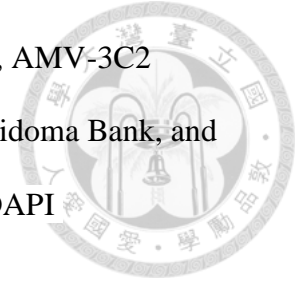
2.4 Tissue total RNA isolation

In anterior dorsal (AD) skin regions, the square of four feather buds in length and three feather buds in width was dissected. In posterior dorsal (PD) skin regions, the square of five feather buds in length and two feather buds in width was dissected (Figure 4A). The dissected skin was immersed at 4℃ overnight for penetration by RNALater solution (Ambion) and then stored at −20°C before isolation of total RNA. After thawing, the samples were homogenized by MagNA Lyzer (Roche). Total RNA was extracted using the MasterPure Complete DNA and RNA Purification kit (Epicentre). The 30 min DNase1 treatment was carried out at room temperature as described in the manual to remove the DNA thoroughly.

2.5 Quantitative PCR

To quantify the candidate gene expressions, the cDNAs were synthesized from the total RNA by QuaniTect Reverse Transcription kit (Qiagen). Each cDNA sample containing SYBR green (KAPA SYBR FAST qPCR kit) was run on LightCycler 480 (Roche) at annealing temperature 63℃ for 45 cycles. Quantification of the TATA box binding protein (TBP) RNA was used to normalize target gene expression levels. All the PCR primers are listed in Table A1.

2.6 mRNA whole mount *in situ* hybridization

Gene-specific fragments were amplified from RNA extracted from dorsal skins of chicken and zebra finch embryos and subsequently cloned into pGEM-T Easy vector

system (Promega, A1360). Both antisense and sense RNA probes were made by in vitro transcription according to manufacture's instructions (Roche, Cat #11277073910). Whole mount *in situ* hybridization was performed using non-radioactive *in situ* hybridization according to the procedure described in Chuong et al. (Chuong, et al. 1996). PCR primers for the cDNA amplifications are listed in Table A2.

2.7 Stranded RNA sequencing

At E8, E9, and E12 zebra finch, the skin total RNAs were pooled from 7, 5, and 3 individuals, respectively. Total RNA concentrations from six libraries (E8A: E8 anterior dorsal skin; E8P: E8 posterior dorsal skin; E9A: E9 anterior dorsal skin; E9P: E9 posterior dorsal skin; E12A: E12 anterior dorsal skin; E12P: E12 posterior dorsal skin) were measured by Qubit fluorometer (Invitrogen USA), and quality was assessed by BioAnalyzer 2100 RNA Nano kit (Agilent, USA). The Illumina library construction and sequencing was conducted by High Throughput Genomics Core of the Biodiversity Research Center, Academia Sinica, Taiwan.

2.8 Data processing and reads mapping

Low-quality bases and reads were removed by using Trimomatic version 0.30 (Bolger, et al. 2014) according to the following procedure: (i) remove adaptors, (ii) remove leading and trailing bases with Phred quality score smaller than 20 (Ewing and Green 1998), (iii) scan the read with a 4-base wide sliding window, cutting when the average Phred quality score per base drops below 20, and (vi) eliminate trimmed reads below 36 bases long. In addition, I trimmed all the paired-end sequencing reads from both ends of each cDNA fragment to 99 bp to reduce sequencing errors.

The zebra finch genome (version Taeniopygia_guttata.taeGut3.2.4) and its gene annotations were downloaded from Ensembl FTP. The processed sequencing reads were

11

mapped to the genome using Tophat version 2.0.8 (Trapnell, et al. 2009), and its

embedded aligner Bowtie version 2.1.0 (Langmead, et al. 2009) with the following

parameters: -N 3 --read-edit-dist 3 --no-novel-juncs --library-type fr-firststrand. The

normalized expression levels of genes, represented by fragments per kilobase of exon

per million fragments mapped (FPKM) (Mortazavi, et al. 2008), were generated by

Cufflinks version 2.1.1 (Trapnell, et al. 2013) with the following parameters:

--max-bundle-frags 10^{12} --multi-read-correct --library-type fr-firststrand.

2.9 Clustering analysis and identification of differentially expressed genes

A gene is said to be expressed if its FPKM value is higher than 1 in at least one of

the six transcriptomes. The Pearson correlation coefficient (PCC) between the 6

expression profiles of the genes was used as the distance metric for gene expression

differences (PCC > 0.8). All expressed genes were hierarchically clustered by the

WPGMA (Weighted Pair-Group Method with Arithmetic mean) method using

heatmap.2 function in the "gplots" package of R (Warnes, et al. 2009). The cut-off for

the cluster analysis is given in Figure A1. I identified the differentially expressed genes

(DEGs) through three sets of comparisons. Gene expressions between AD and PD skin

samples in E8 and E9 libraries were compared. To increase the power of detecting the

DEGs with low expression, the transcriptomes of E8 and E9 AD skins were used as the

AD replicate, while the transcriptomes of E8 and E9 of PD skins were used as the PD

replicate. These two replicates were compared (E8A+E9A versus E8P+E9P). Here we

skipped the samples in E12 because the natal down growth was stopped at E12.

The DEGs from the comparisons were computed by NOISeq (Tarazona, et al.

2011). Only the genes with $q > 0.7$ (odds value) were defined as DEGs (Liu, et al.

2013).

12
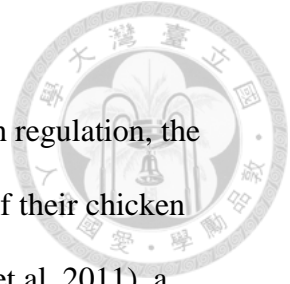
2.10　Gene set enrichment and pathway analysis

To search the possible pathways involved in natal down growth regulation, the Ensemble gene ID of the expressed genes were converted to the ID of their chicken homologs and input into g:Profiler (Reimand, et al. 2007; Reimand, et al. 2011), a web-based toolset for functional profiling of gene lists from large-scale experiments. Biological process, cellular component, molecular function, reactome and human phenotype were used as the dataset. The *p*-value of the gene enrichment was corrected by Benjamini-Hochberg FDR (false discovery rate). Only the gene ontology with the corrected *p*-value < 0.05 was used in further analyses.

2.11　Functional studies

For the generation of proviral constructs, full-length cDNA PCR products were cloned into the pCR8/GW/TOPO Gateway entry vector (Invitrogen, Carlsbad, CA) and sequenced. The cDNAs were transferred into a Gateway compatible RCASBP-Y DV vector through an LR recombination reaction (Loftus, et al. 2001). Virus was made according to Chuong et al. (Chuong 1998) concentrated by ultra-centrifugation. For an *in vivo* assay, RCAS virus directing the expression of the candidate genes was injected into the leg or anterior dorsal skins in E3 chicken embryos. Samples were harvested at E12. At least three independent experiments were conducted for each candidate gene. The primer pairs for the full-length coding sequence amplification were listed in Table A3.

13

3 Results

3.1 Two types of natal down formation in zebra finch embryos

In zebra finch hatchlings, the anterior dorsal, alar, caudal and ventral regions are naked, while the posterior dorsal, capital, humeral, and femoral regions are partially covered by natal down (Figure 4, Figure A2). In chicken hatchlings, the skin is covered by natal down. I compared the natal downs of zebra finch and chicken and found that they share similar nodes and branches (Figure 5), suggesting that they are homologous. However, the natal down of zebra finch is softer and looser than that of chicken.

To characterize the naked and downy tracts in zebra finch, I studied the feather development in zebra finch hatchlings. I focused on the dorsal tract because it showed discrete feather formation. In the anterior dorsal tract and two flanks of the posterior dorsal tract, the feather development does not go through the natal down stage, and the contour feathers develop directly from the feather buds around D7 (Type I, open circles in Figure 4A,B, Figure A2). In contrast, in the middle stripe of the PD tract and other regions labeled with black circles the feather buds formed natal down before the growth of the contour feathers, same as the natal down formation process in chicken (Type II, solid black circles in Figure 4A,B; Figure A2).

To study the developmental differences between Type I and Type II feather buds, I compared the AD and PD regions at different stages of zebra finch and chicken embryos. In E8 zebra finch, all AD and PD tracts formed feather buds (Figure 4C-G). In E9 zebra finch, the growth of Type I feather buds was suppressed (Figure 4I,J), whereas Type II feather buds kept elongating (Figure 4K,L). In E12 zebra finch, Type I feather buds invaginated into the skin but did not elongate (Figure 4N,O), whereas the Type II feather buds invaginated into the skin and elongated (Figure 4P,Q). The phenotype of

14

Type II feather buds in E12 zebra finch was similar to that of the AD and PD feather buds in E12 chicken; that is, the natal downs were keratinized, pigmented and elongated (Figure 4T-X). Furthermore, in newborn zebra finches, the feather buds in the AD region developed follicle structure, but did not protrude out of the skin (Figure 4R,S). Compared to hatchling chicken embryos (Figure 4Y,Z), the down feather in the zebra finch AD region already reached the resting phase.

15

▲

Figure 4. The morphologies and paraffin sections of dorsal natal down in zebra finch and chicken. (A) Dorsal view of the feather tracts in a zebra finch hatchling. Open circles and black circles denote feather buds. (B) Type I (open circles) and Type II (black circles) feather formations. (C-Q) The morphologies and the paraffin sections with H&E staining of the natal downs in AD (Type I) and PD (Type II) skins in E8 (C-G), E9 (H-L), E12 (M-Q), and D1 (R and S) zebra finch. (R) Red arrow indicates the AD region for the section in (S). (T-Z) The morphologies and the paraffin sections with H&E staining of the natal downs in AD and PD skins in E12 (T-X) and D1 (Y and Z) chicken. (Y) Red arrow indicates the AD region for the section in (Z). AD: anterior dorsal skin; PD: posterior dorsal skin; ep: epithelium; me: mesenchyme; fb: feather bud; ff: feather follicle; MDF: mature downy feather. (C, H, M, R, T) Scales bar: 2 mm, other scale bars: 100 μm.
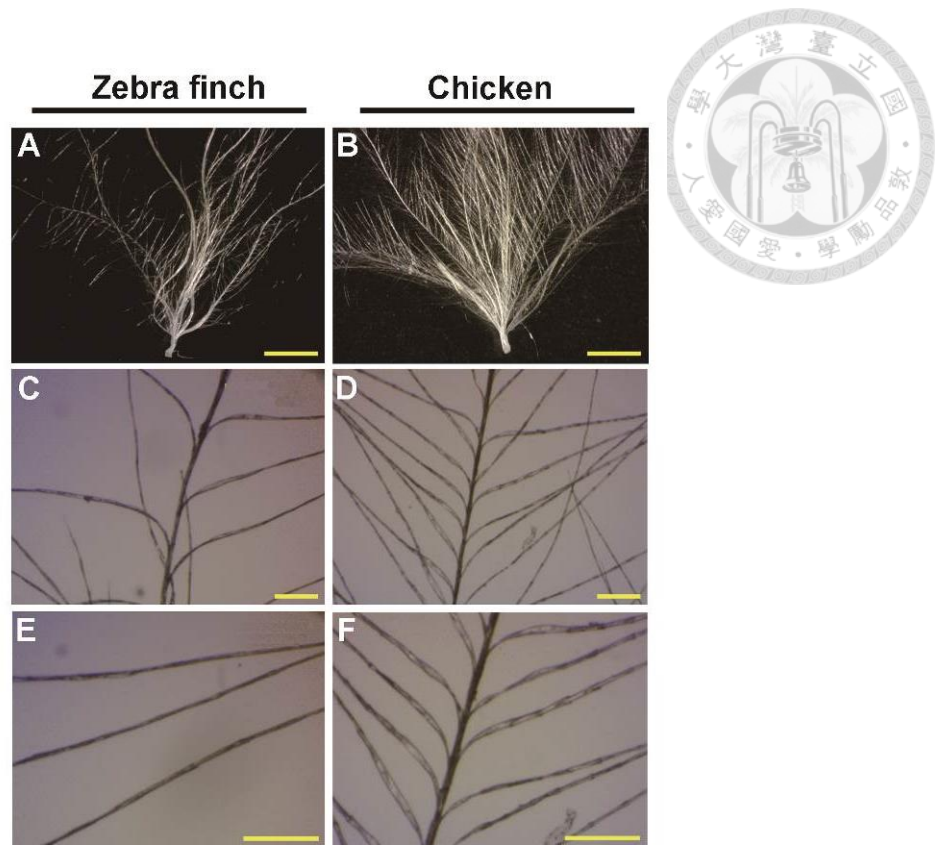
Figure 5. Enlargements of natal downs of zebra finch and chicken. Although the natal down morphology is thicker in chicken than in zebra finch, they share similar branches and nodes in the basic structures. Scales bar: 1 mm in A, B, 100 μm in C-F.

3.2 Anterior dorsal interbud region thickening

To dissect the phenotypic differences between zebra finch and chicken dorsal skins, paraffin sections were made to compare the histological differences. In E12 zebra finch embryos, the epithelium of interbuds in the AD skin (Figure 4N,O), where Type I feathers were formed, was significantly thicker than that of the PD skin (Figure 4P,Q), where Type II feathers were formed (AD: 21.29 ± 0.51 μm vs. PD: 12.96 ± 2.27 μm, $p < 0.05$, Student's t-test). In contrast, no significant difference could be detected between AD (Figure 4U,V) and PD skins (Figure 4W,X) in E12 chicken embryos (AD: $8.75 \pm$

18

0.38 μm vs. PD: 8.71 ± 0.59 μm, $p > 0.05$, Student's t-test). Moreover, the dorsal epithelia were, on average, thicker in zebra finch than in chicken ($p < 0.05$, Student's t-test, Figure 6).
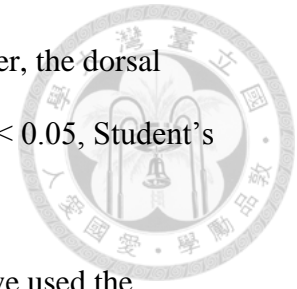
To understand the temporal changes in feather development, we used the immunostaining with PCNA (proliferating cell nuclear antigen) to detect the cell proliferation regions. In AD and PD sections of zebra finch and chicken embryos at E8, E9, and E10, the PCNA signals were enriched in the epithelia of interbuds and feather buds, indicating high cell proliferation in these regions (Figure 7). In E8 and E10, the cell arrangements of interbuds were similar between AD and PD skins in both zebra finches and chickens (E8, Figure 7A-D; E10, Figure 7M-P). In E9 zebra finches, however, the epithelia of AD interbuds showed an irregular cell arrangement compared to those of PD interbuds (Figure 7E,I vs. F,J). No such divergence pattern could be detected in the same regions of E9 chicken embryos (Figure 7G,K vs. H,L). The data also showed higher PCNA signals in the epithelia of PD feather buds in E9 and E10 zebra finches (Figure 7Q) and in that of AD interbuds in E9 zebra finches (Figure 7S), while no significant difference could be detected between the two regions of chicken embryos (Figure 7R,T). To confirm the results, I used the immunostaining with the epithelia cell marker CDH1 (E-cadherin) in the zebra finch paraffin sections. Consistent with PCNA staining, the epithelia of interbud regions were thicker in AD skins than in PD skins (Figure 8). From these histological studies, we conclude that Type I and II feather formations in zebra finch embryos undergo different growth regulation. Type I feather buds skip the elongation and downy steps, suggesting that growth suppressors exist in Type I feather buds in zebra finch embryos.

19
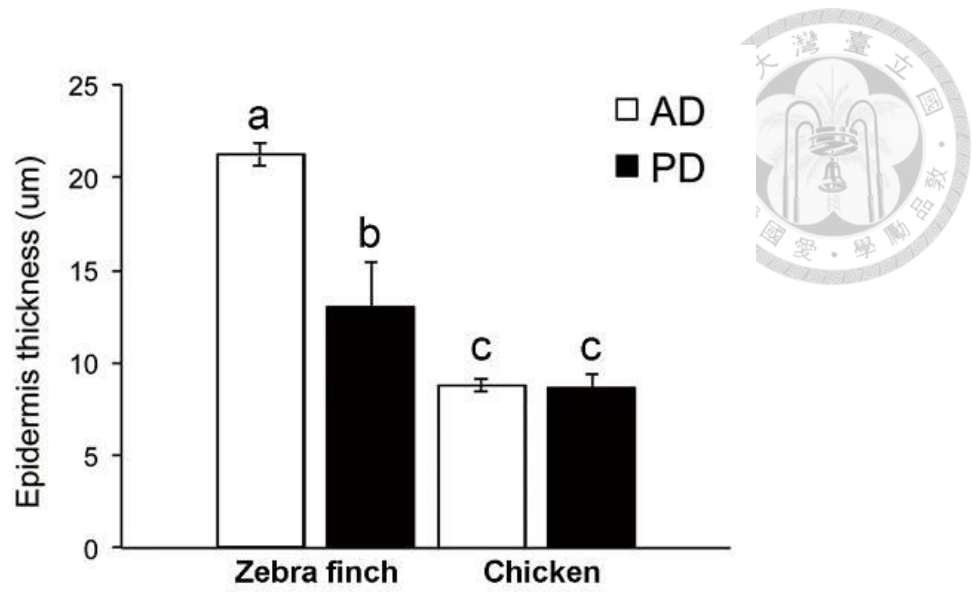
Figure 6. Quantification of the epithelium thickness in AD and PD skins in zebra finch and chicken. AD: anterior dorsal skin; PD: posterior dorsal skin; $p < 0.05$ (Student's *t*-test).

▲
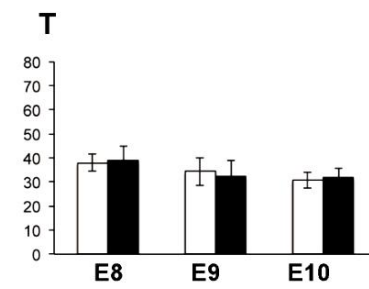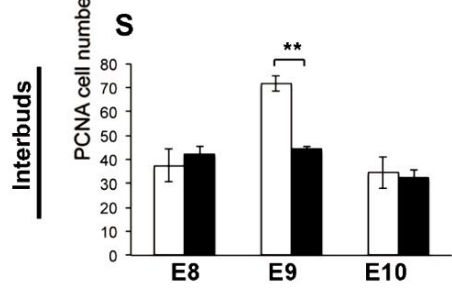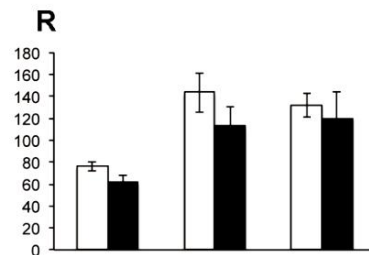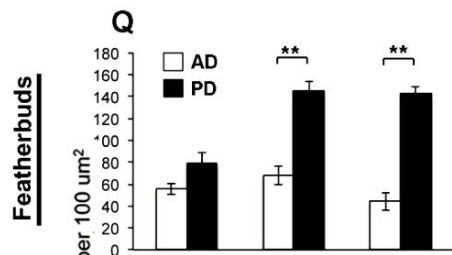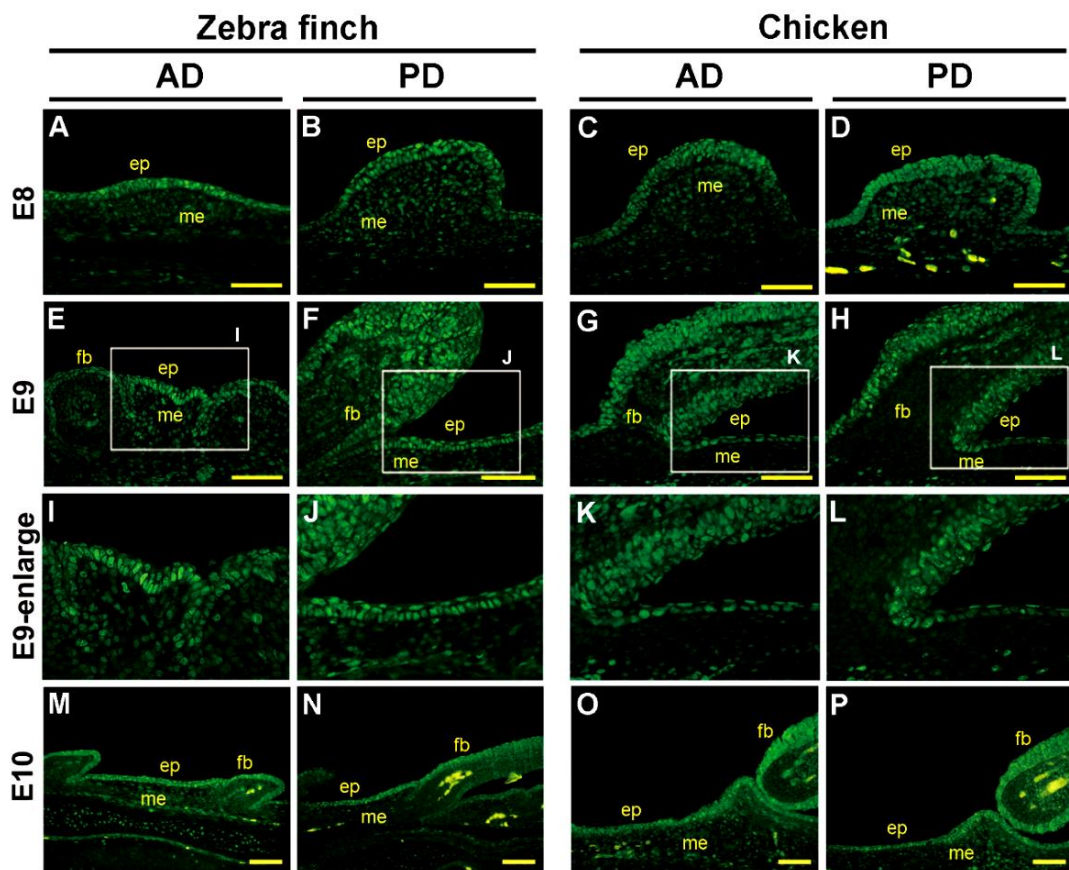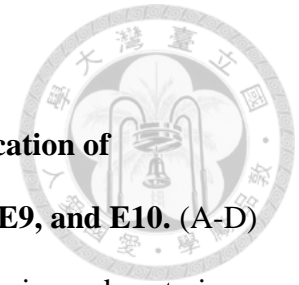
Figure 7. Paraffin sections with PCNA staining and the quantification of proliferating cells in chicken and zebra finch dorsal skins at E8, E9, and E10. (A-D) The anterior and posterior dorsal skin of E8 embryos. (E-H) The anterior and posterior dorsal skin of E9 embryos. (I-L) The enlargement of interbud regions of E-H. (M-P) The anterior and posterior dorsal skin of E10 embryos. (Q-T) Statistics of the proliferating cells in the epithelium of dorsal skins of zebra finch and chicken. (Q, R) The PCNA cell number per 100 μm square in feather buds of zebra finch and chicken at E8, E9, and E10. (S, T) The PCNA cell number per 100 μm square in interbuds of zebra finch and chicken at E8, E9, and E10. Scale bar: 50 μm. AD: anterior dorsal skin; PD: posterior dorsal skin; ep: epithelium; me: mesenchyme; fb: feather buds; **: $p < 0.01$ (Student's t-test).
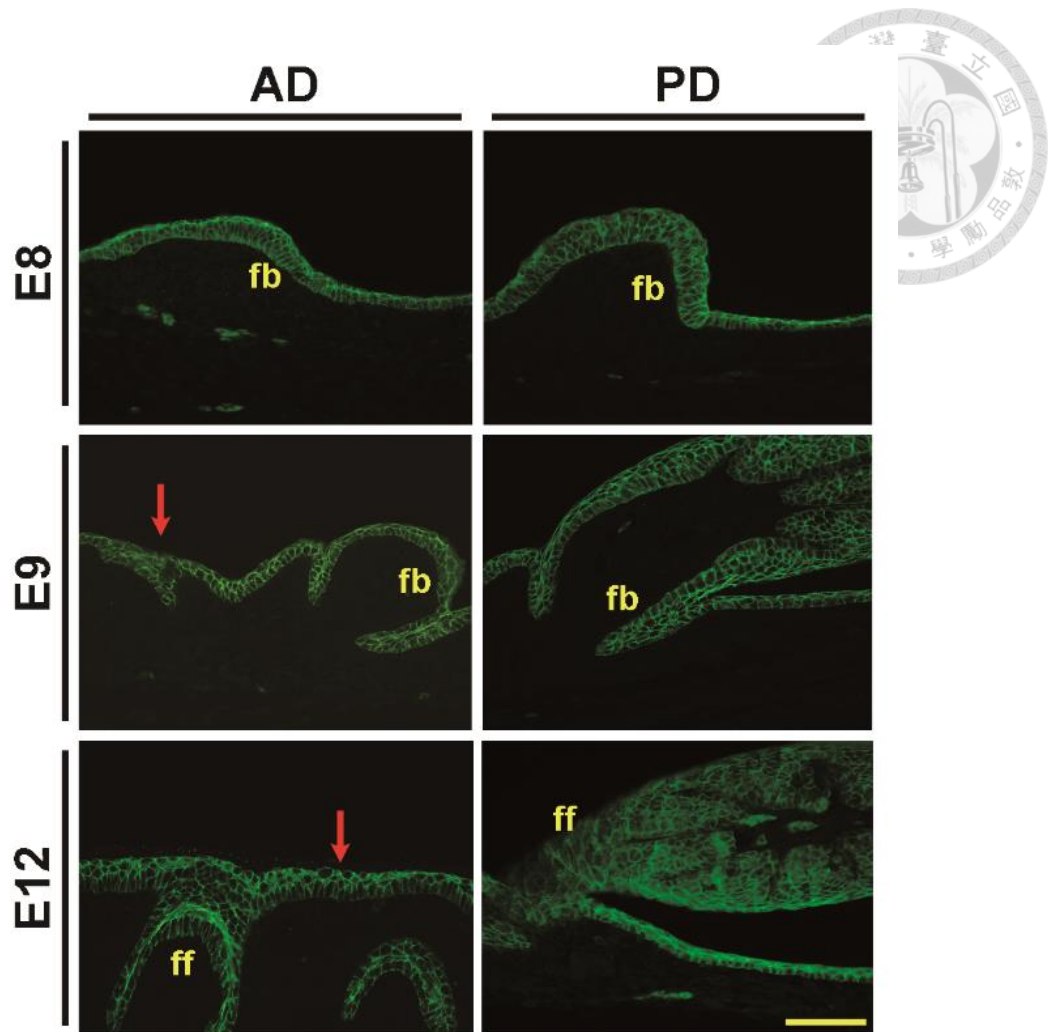
Figure 8. Immunohistochemical stain with CDH1 in paraffin sections of zebra finch dorsal skins. Results showed thickened interbud regions in anterior dorsal skins at E9 and E12 (Red arrow). AD: anterior dorsal skin; PD: posterior dorsal skin; fb: feather bud; ff: feather follicle. Scales bar: 50 μm.

3.3 Transcriptomes of AD and PD regions

To identify the regulatory differences between Type I and II feather formations, I dissected the AD and PD skins of zebra finch embryos at E8, E9, and E12, and obtained six transcriptomes (E8A, E8P, E9A, E9P, E12A, and E12P), using RNA-seq. The sequencing reads from the 6 transcriptomes were mapped to the zebra finch genome (the statistics of sequencing reads are given in Table 2). Among the 18,619 annotated genes, 13,362 had a FPKM value > 1 in at least 1 transcriptome, and they were defined as expressed genes. To evaluate the reliability of RNA-seq data, I measured the expression level of 40 randomly selected genes by the Nanostring technology (Geiss, et al. 2008). A high correlation between RNA-seq and Nanostring data suggested high reliability of the RNA-seq data ($R^2 = 0.83 \sim 0.89$, Figure 9).

Hierarchical clustering analysis clustered the 13,362 expressed genes into 14 clusters (Figure 10). For the 6 transcriptomes, three clusters were formed for the three embryonic stages, i.e., transcriptomes E8A and E8P in one cluster, transcriptomes E9A and E9P in another cluster, and transcriptomes E12A and E12P in a third cluster, suggesting that regional differences in gene expression profiles were smaller than developmental stage differences (Figure 10).

24
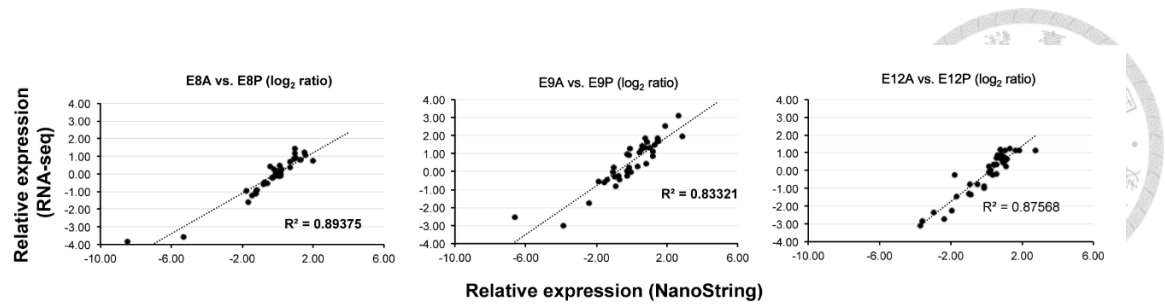
Figure 9. Correlations of gene expressions measured by RNA-seq (x axes) and Nanostring (y axes) of 40 randomly chosen genes. The relative expression differences were calculated as the $\log_2$ fold changes between AD and PD transcriptomes at E8, E9 and E12.
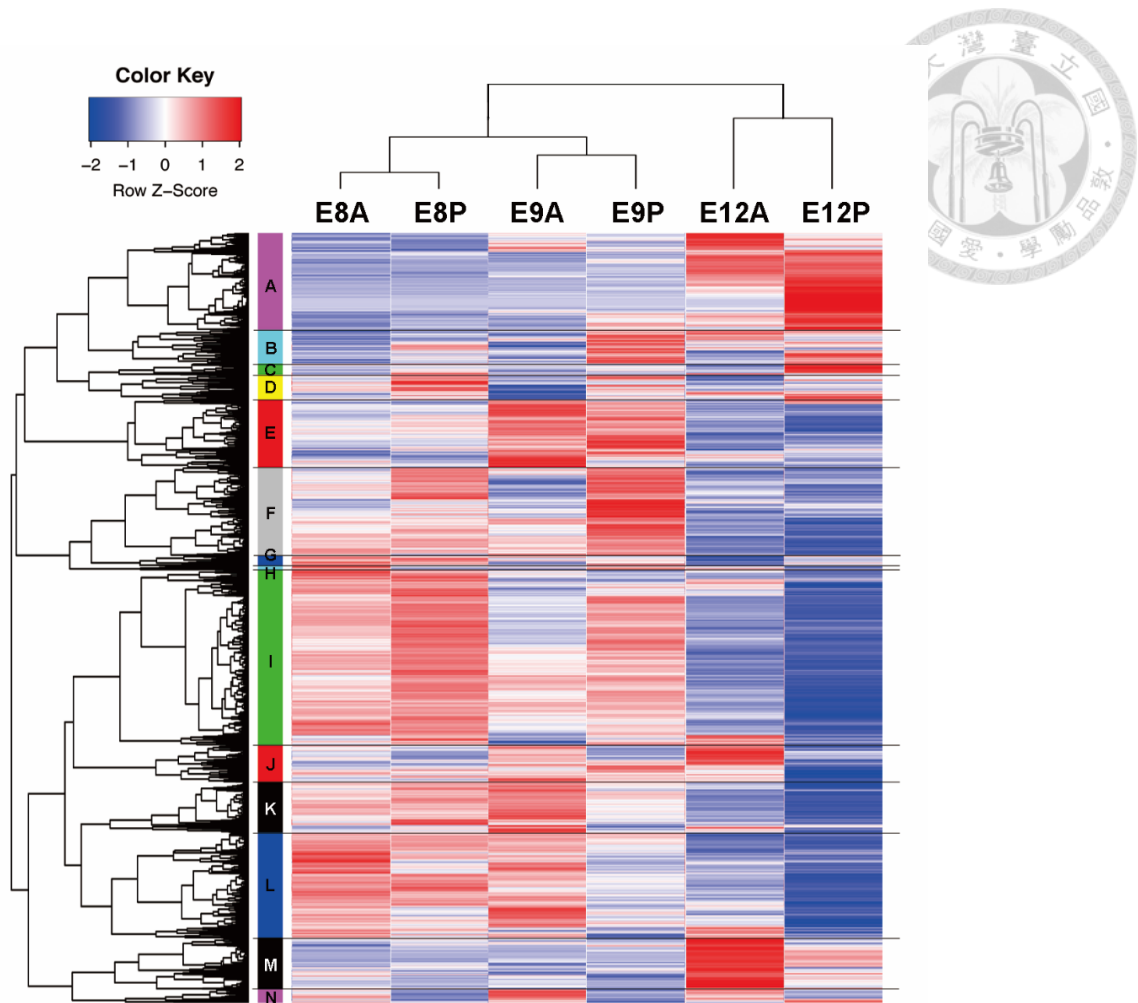
Figure 10. Clustering analysis of the transcriptomes and the expression heat map.

Hierarchical clustering analysis clustered the 13,362 expressed CDSs into 14 clusters (A-N, see Appendix Tables for details). The expression values of each gene are shown as the scaled FPKM values across the six transcriptomes (scaled z-score: red = up-regulation, blue = down-regulation).

The whole set of gene ontology analysis results of clusters are in the link below:

http://mbe.oxfordjournals.org/content/early/2016/04/26/molbev.msw085/suppl/DC1
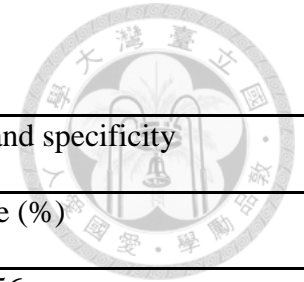
Table 2. Read count statistics of the Illumina deep sequencing data for the 6 libraries studied.

Library	Type	Quality filtering		Mappable reads		Strand specificity
		Total reads	Rate (%)	Filtered reads	Rate (%)	Rate (%)
E8A	101nt, PE	212,574,848	90.0	192,135,468	77.2	89.56
E8P	101nt, PE	195,347,384	90.9	177,704,990	78.2	89.51
E9A	101nt, PE	209,108,402	89.9	187,884,810	76.3	88.87
E9P	101nt, PE	243,286,006	90.2	219,415,584	79.3	86.87
E12A	101nt, PE	238,270,682	90.0	214,572,150	77.2	89.15
E12P	101nt, PE	179,208,508	89.9	161,249,104	78.2	92.84

Note: PE: paired-end.

27
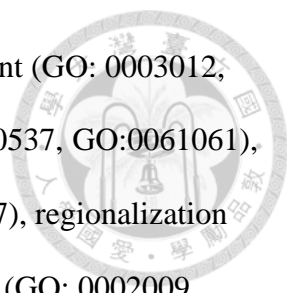
3.4 Clusters of gene expression profiles and their functional enrichments

To have a good statistical power for gene clustering analysis, I selected and analyzed the clusters with more than 500 genes and with higher than 5% DEGs (Table 3).

The clusters with genes expressing higher in PD than in AD may include natal down growth promoters. Cluster A included most of the expressed feather and scale keratin genes and genes with a higher expression level in E12 than in E8 and E9 (Figure 10; Table A4). GO categories were enriched in intermediate filament and cytoskeleton (GO:0005882, GO:0045111, GO:0005200), hyperpigmentation (GO: 0001010, GO: 0001053), and abnormality of skin morphology (HP: 0011121, HP: 0011122, HP: 0008065) (Table A5). Cluster B included genes with a higher expression level in PD transcriptomes than in AD transcriptomes at all three stages (Figure 10). GO categories were enriched in toll-like receptor signaling pathway (GO: 0034138,GO: 0034123) and cytolysis (GO: 0019835) (Table A6). These enrichments could be due to regional innate immune responses to the skin dissection. Cluster F included genes with a higher expression level in E8 and E9 than in E12 (Figure 10). E8 and E9 were the stages of feather bud elongation, and the GO categories were enriched in gene expression (GO: 0010467), biosynthetic process (GO: 1901576, GO: 0009059), nucleic acid binding (GO: 0003676, GO: 0003723) (Table A7), suggesting that feather bud elongation is subjected to complex gene regulation. Two known feather growth promoters, *SHH* and *MSX1*, in this cluster had a significantly higher expression level in PD than in AD, reflecting their important roles in zebra finch natal down development (Table A4).

In contrast, the clusters with genes expressing higher in AD than in PD may include natal down growth suppressors (Figure 10). In Clusters J, M, L and N, GO

28

categories were enriched in muscle component or muscle development (GO: 0003012, GO: 0043292, GO: 0044444, GO: 0005581, GO: 0005861, GO:0060537, GO:0061061), organismal development (GO: 0032501, GO: 0007275, GO: 2000027), regionalization (GO: 0048856, GO:0003002, GO: 0051674), epithelial development (GO: 0002009, GO: 0050678), and MAPK signaling pathway (KEGG:04010) (Table A8 to A11).

However, the results might be affected by our sampling bias: First, the AD skin tended to adhere to the muscle tissue beneath, and muscle development related genes might therefore be enriched in our analysis. Second, the AD and PD regional dissections might increase the detection of regional-specific genes. To identify the GO categories potentially responsible for natal down growth suppression, we chose the DEGs that are most frequently present in the GO categories and compared their chicken homologous gene expressions between chicken AD and PD skins at E8 and E9 by quantitative PCR. *ACTA1*, *ACTC1*, *CHRNA1*, *MYOD*, *MYOG* and *TNNC1*, which were most frequently present in the GO categories of muscle development, showed the same expression patterns in zebra finch and chicken (Figure 11). Similarly, *HOXBs* and *HOXCs*, which were most frequently present in the GO categories of organismal development and regionalization, showed the same expression patterns in zebra finch and chicken (Figure 11). These DEGs are unlikely to be responsible for natal down growth suppression.
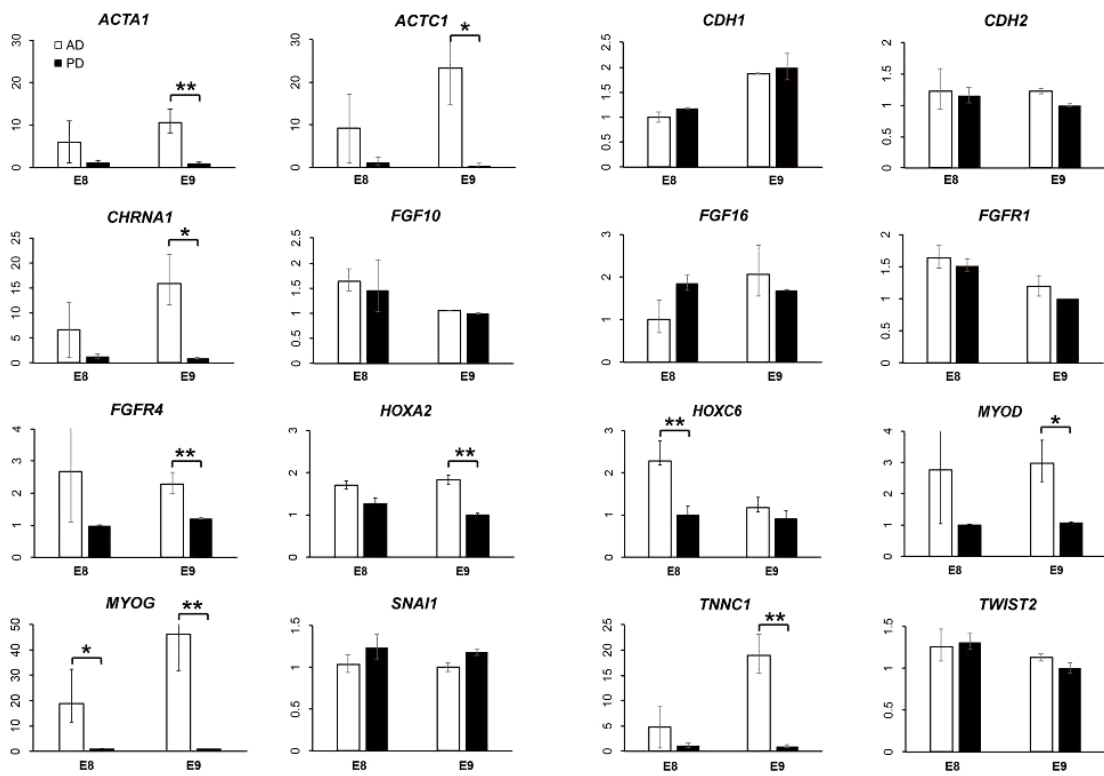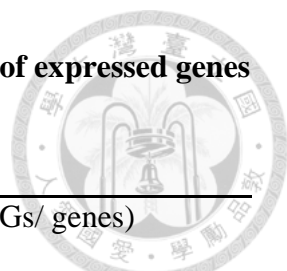
Figure 11. Quantitative PCR of candidate genes in chicken AD (white bar) and PD (black bar) skins at E8 and E9. AD: anterior dorsal skin; PD: posterior dorsal skin.

*: $p < 0.05$; **: $p < 0.01$ (Student's *t*-test).

30

Table 3. The clusters of gene expression profiles and the number of expressed genes and the number of DEGs in a cluster.

Clade	Gene number	DEGs	Ratio (DEGs/ genes)
A	**1677**	**128**	**7.6 %**
B	**585**	**54**	**9.2 %**
C	194	5	2.6 %
D	429	20	4.7 %
E	1180	23	1.9 %
F	**1534**	**93**	**6.1 %**
G	176	3	1.7 %
H	68	8	11.8 %
I	3046	20	0.6 %
J	**639**	**74**	**11.6 %**
K	875	10	1.1 %
L	**1829**	**125**	**6.8 %**
M	**891**	**42**	**4.7 %**
N	**239**	**70**	**29.3 %**

Note: The bold letters indicate the clusters with more than 500 genes and higher than 5% DEGs.

31

3.5 Differential *SHH* expression between Type I and II feather formations

Cluster F showed genes expressing higher in PD than in AD and may include natal down growth promoters (Figure 10). SHH is a known important feather growth promoter and I therefore considered SHH a factor for growth divergence between Type I and II feather formations. To study the expression profile of *SHH* in the zebra finch embryos, I quantified its expression levels at different embryonic stages. Quantitative PCR data showed *SHH* differentially expressed between AD and PD skins at E9 and E10 (Figure 12A). The differential expression disappeared at E12, when the natal down elongation was completed (Figure 12A).

To visualize the differential expression of *SHH* between Type I and II feather buds, whole mount *in situ* hybridization was conducted in the E9 zebra finch embryos, using *β-catenin*, a known initiation signal for feather bud formation (Noramly, et al. 1999) and with little differential expression in our transcriptomes (Table S4), for the experimental control (Figure 12B-D). In E9 zebra finch embryos, the expression of *SHH* was restricted to the posterior end of the Type II feather buds (Figure 12E,G), the same as that in chicken feather buds (McKinnell, et al. 2004), suggesting that chicken and zebra finch share homologous natal down. However, Type I feather buds showed a lower level of *SHH* expression than Type II feather buds (Figure 12F vs. G). Moreover, in Type I feather buds of E10 zebra finch embryos, the expression of *SHH* lost its regular posterior polarity (blue arrows in Figure 12F,I), implying that the function of SHH was disrupted in feather bud elongation.
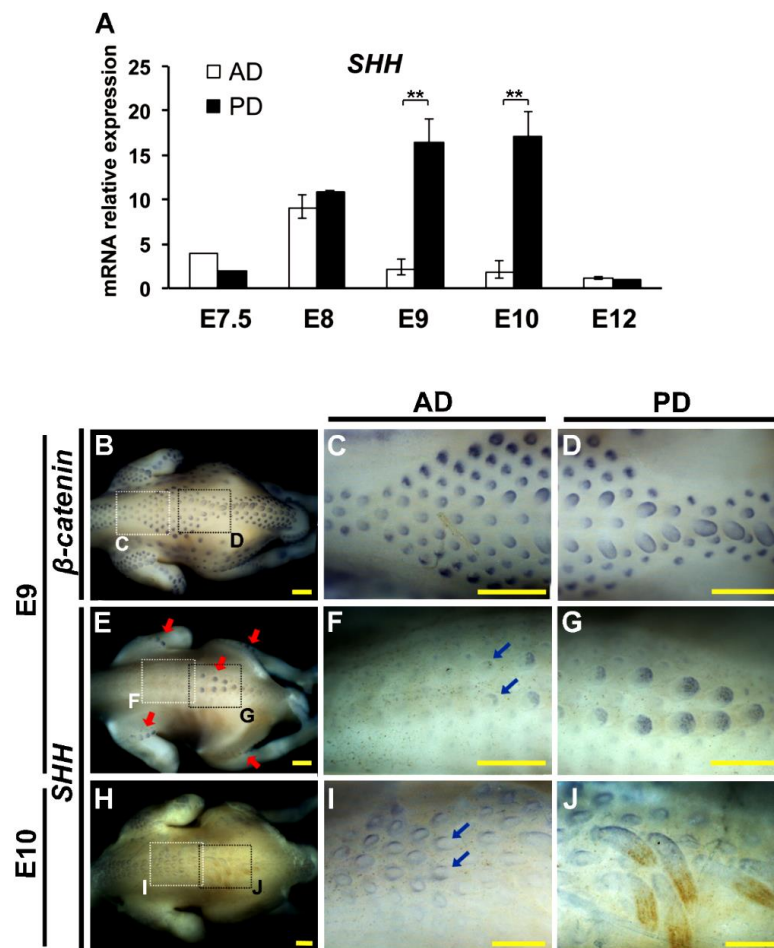
Figure 12. Differential expression of *SHH* between Type I and Type II feather formations in zebra finch. (A) Quantification of *SHH* mRNA expression of AD and PD skin regions at different embryonic stages. Relative expression values were given in mean ± SD from at least three independent experiments. **: $p < 0.01$ (Student's *t*-test). (B-J) Whole mount *in situ* hybridization of *β-catenin* and *SHH* in zebra finch embryos. (B-D) *β-catenin* in E9 embryos. (E-G) *SHH* in E9 embryos. (H-J) *SHH* in E10 embryos. The enlargements of anterior and posterior dorsal skins were indicated by the white (C, F and I) and black dotted-line (D, G and J) squares in B, E and H. Red arrows indicate the expression locations of *SHH*. Blue arrows indicate the disruptive expression patterns of *SHH*. Scale bar: 0.5 mm.

33

3.6 FGF16 suppresses natal down growth and thickens the epithelium through the FGF/MAPK pathway

From the above transcriptome analysis, I noted that *FGF10*, *SNAI1* and *TWIST2*, which belong to the GO category of epithelial development, showed a higher expression level in AD skin than in PD skin in zebra finch embryos (Cluster L, Figure 10), but the homologs of these genes in chicken showed little differential expression in our quantitative PCR data (Figure 11). The same comment applies to *FGF16*, which is in the GO category of the MAPK signaling pathway (Cluster N, Figure 10).

Among the four candidate genes (*FGF10, FGF16, SNAI1* and *TWIST2*), *SNAI1* and *TWIST2* were two highly expressed genes in the transcriptome and so were selected for whole mount *in situ* hybridization in zebra finch embryos. By whole mount *in situ* hybridization in E9 zebra finch, I found that the expression of *TWIST2* was throughout the dermis of Type I feather buds (Figure 13A,B,D), but was restricted to the anterior proximal dermis of Type II feather buds (Figure 13A,C,E). A similar expression profile was detected in *SNAI1* (Type I feather buds: Figure 13F,G,I; Type II feather buds: Figure 13F,H,J), which is a zinc finger transcription factor for regulating epithelial to mesenchymal transition (EMT) during embryonic development (Paznekas, et al. 1999). These data support the association between our predicted genes and the feather bud growth suppression.

In feather development, the MAPK signaling pathway was shown to be the major downstream pathway in response to FGFs (Lin, et al. 2009). Previous knockout of the key component of the MAPK pathway reduced epithelium thickness in mouse (Scholl, et al. 2007). Thus, it appears that the FGF/MAPK pathway participates in the natal down growth suppression. FGF16 is a known upstream signal of SNAI1 in promoting

34

ovarian cancer cell invasion through activation of the MAPK signaling pathway (Basu, et al. 2014). Therefore, I hypothesized that the up-regulation of *FGF16* in AD skin suppresses natal down growth and increases epithelium thickness.

To test this hypothesis, I utilized the RCAS retrovirus to overexpress the *FGF16* gene in chicken embryos. Because injecting *FGF16* cDNA into the chicken AD skin region caused high lethality (data not shown), I injected it into the legs instead. In each chicken embryo, one leg was injected with the virus carrying the *FGF16* cDNA, while the other leg was used as the control. We found that *FGF16* overexpressed legs exhibited a similar phenotype of the zebra finch AD skin region: periodic feather buds were formed, but natal down elongation was suppressed (Figure 14A,C,E). The natal down elongation in the control leg was normal (Figure 14B,D,F). Moreover, bone formation was also influenced by *FGF16* overexpression (Figure 14A), supporting a previous prediction (Laurell, et al. 2014). In the paraffin sections of the skin, both the H&E stain and the immunostaining with CDH1 showed thicker epithelia in the *FGF16* overexpressed leg skin than in the control leg skin (Figure 14E,G vs. F,H; statistics in Figure 14J). Four independent experiments were conducted for *FGF16* overexpression and three individuals with suppressed natal down were shown in Appendix data (Figure A3).

To understand how FGF16 suppresses natal down elongation, I studied the expression patterns of several genes in *FGF16* overexpressed skins by quantitative PCR. The expression of *FGFR1* was up-regulated, whereas *β-catenin* (*CTNNB1*) and *FGFR4* were not affected by *FGF16* overexpression (Figure 15A). This observation suggests interaction between FGF16 and FGFR1. Although *FGFR1* was not in our list of differentially expressed genes, the transcriptome data showed 1.6 fold higher expression

of *FGFR1* in the AD than in PD skin of E9 zebra finch (Table S4). Moreover, *SNAI1* and *TWIST2* were also up-regulated in the *FGF16* overexpressed skin (Figure 15A), although the differences were not statistically significant. Interestingly, *FGF10* was up-regulated, while *SHH* was down-regulated in the *FGF16* overexpressed skin (Figure 15A).

To test the relationship between FGF10 and FGF16, *FGF10* was overexpressed in the dorsal skins of chicken embryos, resulting in the suppression of the natal down formation (Figure 16A,C vs. B,D), but the expression of *FGF16* was not affected (Figure 16E). These observations suggest that FGF10 is not a regulator but a target of FGF16. Thus, I conclude that FGF16 suppresses the natal down elongation through the FGF/MAPK pathway (FGF10, FGFR1, SNAI1 and TWIST2) and the down-regulation of SHH (Figure 15B).

In addtion to *FGF16* and *FGF10*, I also injected several candidate regulators that expressed higher in AD skin than in PD skin in E8 zebra finch embryos to the dorsal region of chicken; however, only RCAS-*FGF16* and *FGF10* suppressed the natal down elongation. All the tested genes and the microinjection results are shown in the Appendix data (Figure A4).
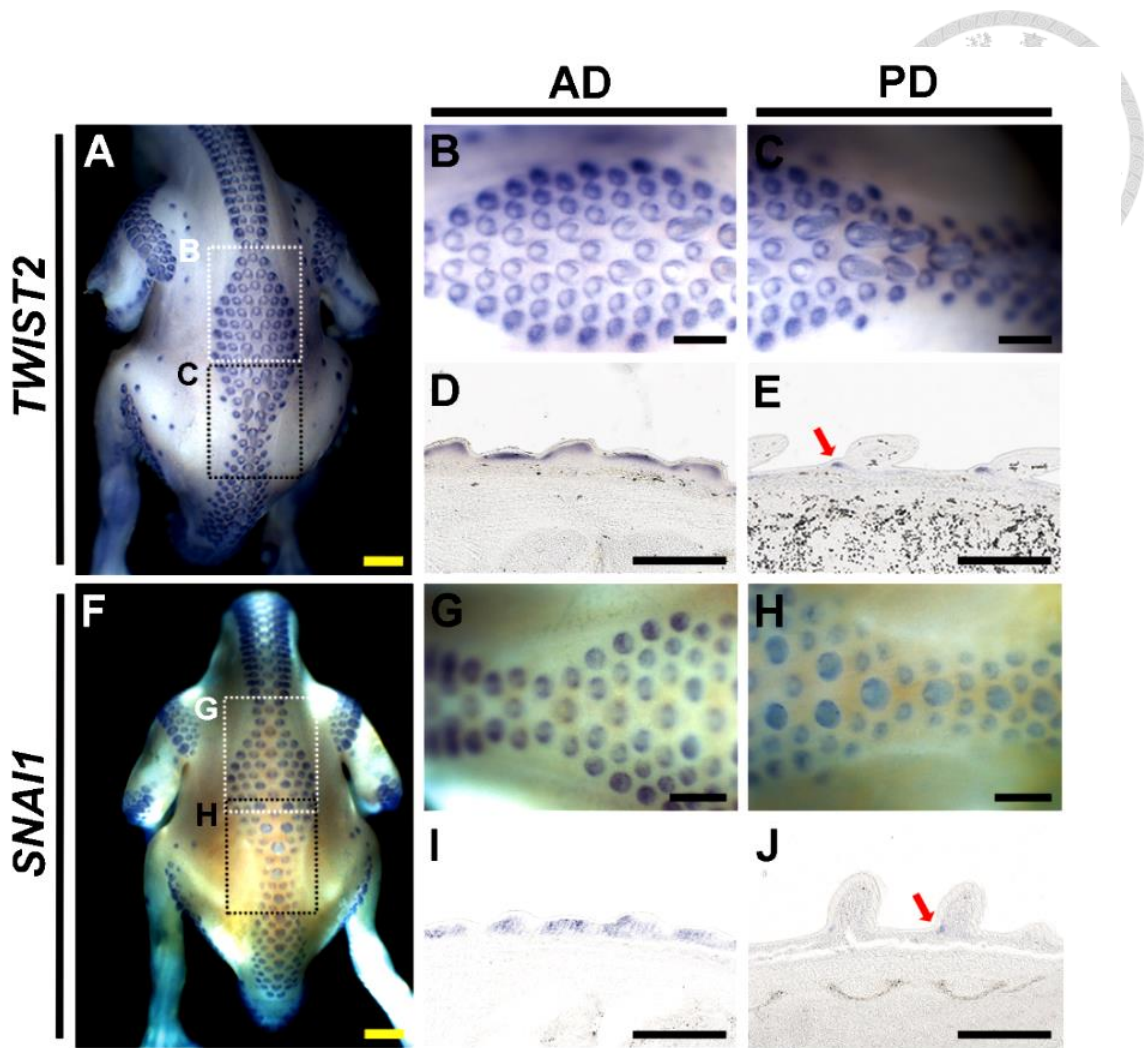
Figure 13. Whole mount in situ hybridization of *TWIST2* (A-E) and *SNAI1* (F-J) in E9 zebra finch and the paraffin sections. (B, C) The enlargements of the dotted-line square regions in (A). (G, H) The enlargements of the dotted-line square regions in (F). (D, E) the paraffin sections of feather buds of B and C, respectively. (I, J) the paraffin sections of feather buds of G and H, respectively. Red arrows indicate the restrictive expression pattern of *TWIST2* and *SNAI1* in Type II feather buds. Scale bar: 0.5 mm.

37

RCAS-FGF16   Control

A   C

B   D

C   leg

D   leg

H&E

E   fb   ep   me

F   fb   ep   me

CDH1

G

H

AMV-3C2

I

J   Epidermis thickness (μm)   □FGF16 ■Control   **

38

▲
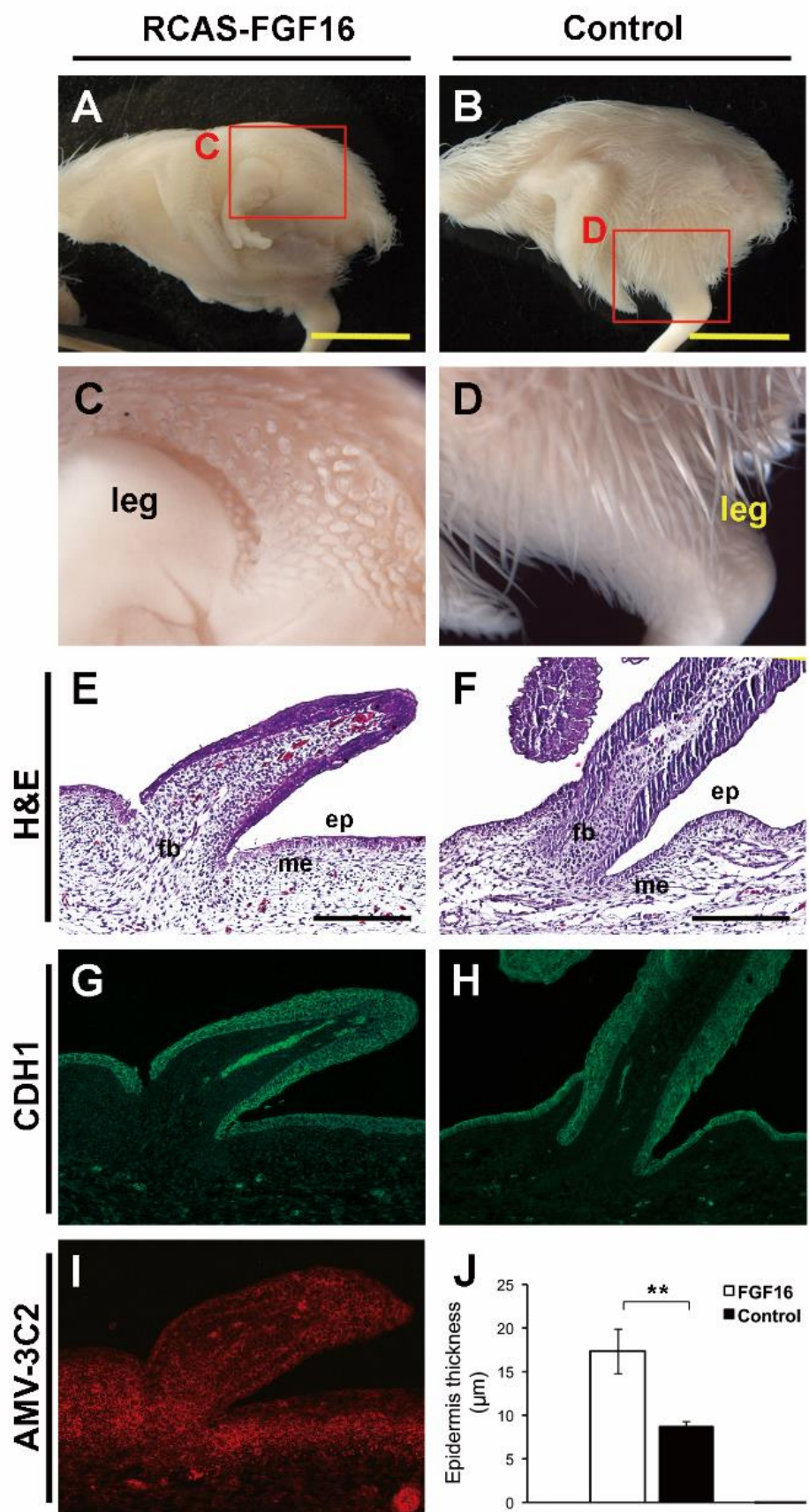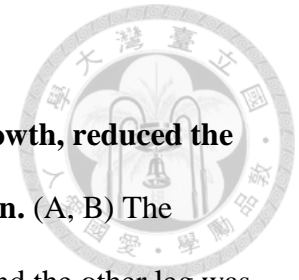
Figure 14. *FGF16* overexpression suppressed the natal down growth, reduced the bone length, and increased the epithelial thickness in E12 chicken. (A, B) The chicken embryo was microinjected with RCAS-FGF16 in one leg, and the other leg was used as the control. (C, D) The enlargement images of Figures A and B, respectively. (E, F) H&E stains of the paraffin sections of *FGF16* overexpressed and control skins. (G, H) Immunochemical stain with CDH1 in the paraffin sections of the *FGF16* overexpressed and the control skins. (I) AMV-3C2 staining of adjacent sections showing the RCAS virus infected regions. (J) Quantification of the epithelium thickness between the *FGF16* overexpressed (white bar) and the control epithelia (black bar). Ep: epithelium; me: mesenchyme; fb: feather bud. **: $p < 0.01$ (Student's *t*-test). Yellow scale bar: 1 cm, black scale bar: 100 μm.
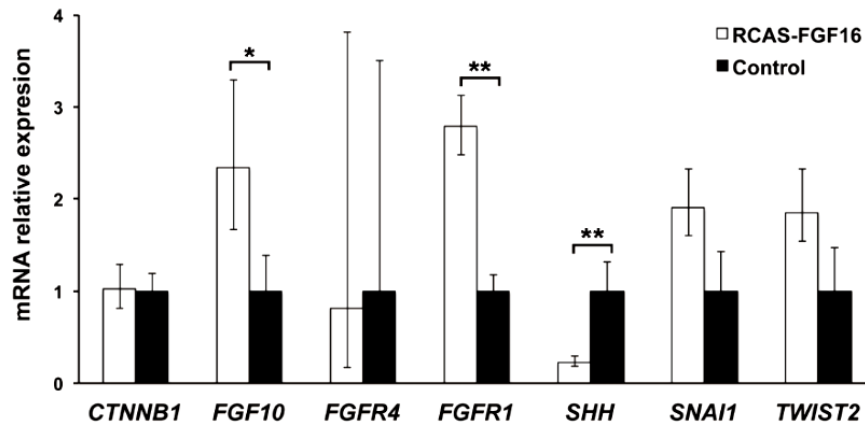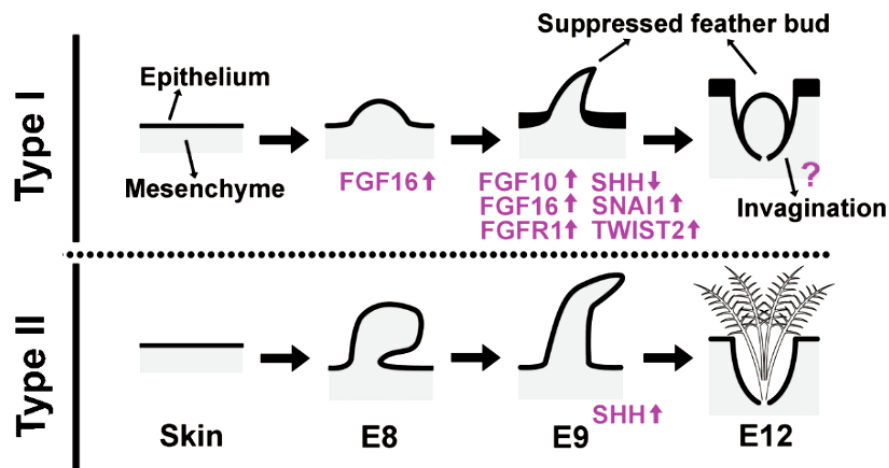
Figure 15. The quantification of the candidate genes for natal down growth suppression, and the summary diagram of Type I and Type II feather formations.
(A) The gene expressions in the *FGF16* overexpressed (white bar) and control (black bar) skins in chicken were compared by quantitative PCR. Relative expression values were given in mean ± SD from at least three independent experiments. *: $p < 0.05$; **: $p < 0.01$ (Student's *t*-test). (B) The summary diagram of Type I and Type II feather formations, and the involved phenotypes (black words) and molecular regulators (pink words).

40
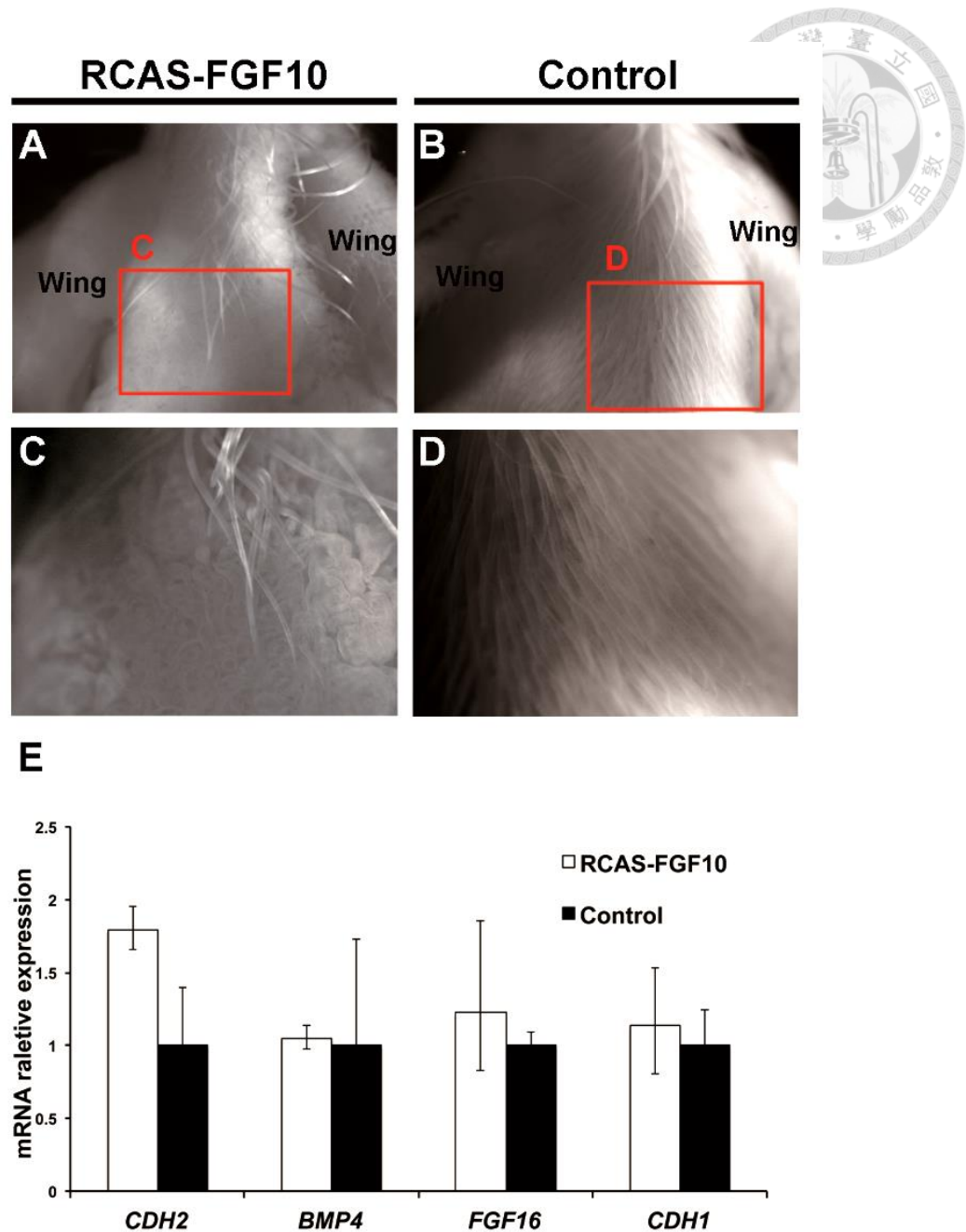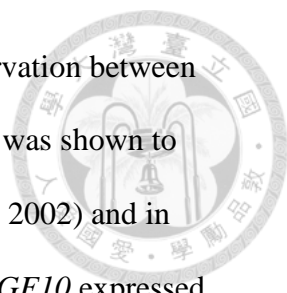
Figure 16. Overexpression of *FGF10* suppressed the natal down growth but had no influence on the *FGF16* expression. (A, B) The control and RCAS-FGF10 microinjected dorsal skin in chicken E12 embryos. (C, D) The enlargements of A, B, respectively. (E) Relative mRNA expression difference between *FGF10* overexpressed and control skin of known feather regulators by quantitative PCR.

41

4 Discussion
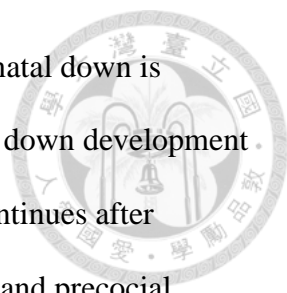
In this study, I first defined two types of natal down formation in the dorsal skin of zebra finch, in contrast to only one type in chicken. The absence of natal down in Type I feather formation signifies the altricial phenotype in zebra finch. Previous studies found that the naked skins in the *sc/sc* and naked neck chicken were due to the abolishment of feather bud formation (Mou, et al. 2011; Wells, et al. 2012). However, in zebra finch hatchlings I found typical feather buds in some regions of the skin (Figure 4), suggesting that a different regulatory mechanism suppresses feather growth. Moreover, according to the expression patterns of *SHH* (Figure 12), the difference between AD and PD skin regions at the developmental stages studied is not due to heterochrony because AD skin never grows natal down. I utilized the comparative transcriptomics approach to infer that molecules in the FGF/MAPK pathway are involved in the natal down growth suppression and epithelial thickening, leading to naked AD skin regions in zebra finch hatchlings.

FGFs are key players in the processes of proliferation and differentiation of a wide variety of animal cells and tissues (Ornitz and Itoh 2001). In feather elongation, FGFs may play two opposite functions. Some, such as FGF2 and FGF4 (Widelitz, et al. 1996; Song, et al. 2004), may induce or promote feather growth, while others, such as FGF10 and FGF16, may play a suppressor role (Tao, et al. 2002; Yue, et al. 2012). Overexpression of *FGF10* thickens the epithelium, up-regulates *NCAM* and down-regulates *SHH*. FGF10 suppresses the chicken natal down growth through the epithelium/mesenchyme signaling interaction (Tao, et al. 2002), leading to a phenotype similar to that in zebra finch AD skin in which periodic feather germs are formed, but feather elongation is suppressed.

42

The natal down growth suppressors showed functional conservation between different skin regions and between avian species. In chicken, FGF10 was shown to suppress the natal down growth in the leg skin previously (Tao, et al. 2002) and in dorsal skin in this study (Figure 16). In my transcriptome analysis, *FGF10* expressed higher in AD skin than in PD skin of zebra finch embryos (Table A4), suggesting a role in natal down growth suppression. On the other hand, *FGF16* expressed higher in AD skin than in PD skin of zebra finch embryos (Table A4), and suppressed the natal down elongation in the leg skin of chicken embryo, suggesting a role in natal down growth suppression in altricial hatchlings. However, due to experimental limitations in zebra finch, I was unable to overexpress or knock down *FGF16* in zebra finch. Furthermore, due to the low expression of *FGF16* in zebra finch (FPKM value 1~8), I found it difficult to distinguish noise from the true signal by *in situ* hybridization. Therefore, I cannot rule out the possibility that the natal down growth was indirectly suppressed due to the wide range of *FGF16* overexpression by the RCAS system. More experimental innovations are needed to address these issues.
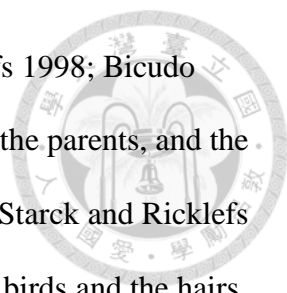
TWIST2 is known to be a feather growth initiator, but overexpression of *TWIST2* induced thickened dermis with normally shaped ectopic feather buds (Hornik, et al. 2005). There are two possible explanations for its role in natal down suppression. First, other molecules such as *SNAI1* that showed coexpression with *TWIST2* may work in a combined action manner. As suggested by a previous study (Oh, et al. 2004), the combined action of modest inhibitors can abolish the function of MAPKs. Moreover, the differential expression of *TWIST2* might be the consequence, but not the cause of feather bud growth suppression. The continued expression of *TWIST2* in Type I feather buds in E9 zebra finch might be due to a pleiotropic effect of *FGF16* overexpression.

43

It should also be pointed out that the developmental process of natal down is diverse among altricial birds. For example, in most finches, the natal down development is finished at hatchlings, but in the parrots, the natal down growth continues after hatching (data not shown). Furthermore, when I mapped the altricial and precocial phenotypes onto the recently published avian phylogeny (Zhang, et al. 2014), I found that the altricial-precocial transition occurred multiple times in the past 70 million years, as previously proposed (Starck and Ricklefs 1998). Although the precocial phenotype is considered ancestral to the altricial phenotype, some precocial orders, such as ciconiiformes and gruiformes, are clustered with altricial lineages, while some altricial orders, such as cuculiformes and apodiformes, are clustered with precocial lineages (Starck and Ricklefs 1998; Zhang, et al. 2014). Thus, different mechanisms may act in the natal down growth regulation in birds. Whether the FGF/MAPK signaling pathway is utilized as the natal down growth suppressor in all altricial birds needs to be investigated.

The feather bud elongation in AD skin of zebra finch embryos stopped at around E9, and the phenotype of the suppressed feather bud is similar to that in *FGF16* overexpressed chicken skins (Figure 4J and Figure 14C). However, the epithelium invagination and feather follicle formation still proceed in the AD skin of E12 zebra finch embryos (Figure 4O), but not in *FGF16* overexpressed chicken skins (Figure 14E). This difference suggests that overexpression *FGF16* may suppress invagination and follicle formation or the FGF/MAPK pathway is not the only factor for natal down growth suppression. More works remain to be investigated to identify the whole regulatory network of altricial feather suppression.

The natal down divergence between altricial and precocial hatchlings is thought to

44

be associated with heat transfer and conservation (Starck and Ricklefs 1998; Bicudo 2010). In altricial hatchlings, most of their body heat is conferred by the parents, and the naked dorsal skin is thought to be associated with heat transduction (Starck and Ricklefs 1998). The cornified epidermal keratinocytes, such as the feathers of birds and the hairs of mammals, are essential for the adaptation of the terrestrial animals (Strasser, et al. 2015). I found that epithelial thickening is a phenotype in featherless AD skin of zebra finch hatchlings. In the naked mole-rat, lack of fur is compensated by a thicker epidermal layer and a marked reduction in sweat glands (Daly and Buffenstein 1998). Similar mechanisms might be shared between these naked organisms for environmental adaptation.

The evolution of feathers was so successful as to enable the birds to become the most diverse amniotes. However, like the recurrent losses of limb or eye in animal evolution (Lande 1978; Protas, et al. 2011), feather evolution is not unidirectional. Fossil records showed that most ancestral birds had flight feathers on their legs, but this phenotype is rare in modern birds (Dhouailly 2009; Zheng, et al. 2013). The loss of the leg flight feather might have enhanced flight ability (Dial, et al. 2008). This study provided another case of feather growth suppression. My view is that the feather growth suppression during Type I feather formation is due to the overexpression of specific suppressors, but not due to the functional loss of the feather growth promoters. The evolution of feather growth suppressors implies feather growth may sometimes lower the species fitness. Furthermore, the saved energy of feather growth can be allocated to the development of other organs, such as the post hatch fast brain growth (Starck and Ricklefs 1998). Together, these evolutionary novelties may have made the passerine birds the most diverse avian species.

45

SUMMARY AND PROSPECTIONS

My major research interest is feather development and evolution. Feather is a unique evolutionary innovation. Feathers are skin appendages but have highly ordered and hierarchically branched structures. Feathers evolved in dinosaurs but underwent dramatic diversification in birds, allowing birds to adapt to various ecological niches. Natal down is the plumage of avian hatchlings and is used to classify birds into altricial and precocial. Signaling molecules involved in natal down development may be associated with the natal down divergence and my study showed that the FGF (fibroblast growth factor)/MAPK (mitogen-activated protein kinase) pathway is involved in natal down growth suppression in zebra finch hatchling (Chen, et al. 2016).

My study provides insights into the regulatory divergence in natal down formation between precocial chicken and altricial zebra finch, but raises questions about bird and feather evolution. The first important question is whether the FGF /MAPK pathway is used by all the naked altricial hatchlings. To answer this question, one needs to understand the evolution of the precocial to altricial continuum. Generally, one avian order only shows one type of developmental mode. I mapped the altricial and precocial phenotypes onto the recently published avian phylogeny (Zhang, et al. 2014) and found that the precocial to altricial transition occurred multiple times in the past 70 million years, as previously proposed (Figure 17) (Starck and Ricklefs 1998; Deeming and Reynolds 2015). Although the precocial phenotype is considered ancestral to the altricial phenotype, some precocial orders, such as Eurypygiformes and Cariamiformes, are clustered with altricial lineages. Some altricial orders, such as Phoenicopteriformes and Mesitornithiformes, are clustered with precocial lineages (Figure 17) (Starck and Ricklefs 1998; Zhang, et al. 2014; Deeming and Reynolds 2015). Thus, the evolution of

46

the precocial to altricial continuum should include multiple independent events and different mechanisms may act in the natal down growth regulation in birds. More investigations of the molecular mechanisms of natal down development in different kinds of birds are necessary to resolve this question.

Second, although the FGF/MAPK pathway had been proposed in natal down suppression in this study (Chen, et al. 2016), I cannot identify the evolutionary change in sequence of or close to *FGF16* between zebra finch and chicken, showing that some regulators may work upstream to FGF16. A recent bioinformatics pipeline developed in our lab that was used to predict the transcription factors of the specific genes depend on gene co-expression and sequence conservation could be used to predict the upstream transcription factors of *FGF16* (Bhattacharjee, et al. 2016).

Third, although the hatchlings of altricial birds are almost naked and those of precocial birds are covered with natal down, most feather follicles (both downy and naked follicles) are replaced by contour feathers when birds are ready to leave the nest in their juveniles (Figure 18) (Podulka, et al. 2004). After several times of moulting, more functional feathers develop from the juvenile feather follicles to achieve specific function in adult birds (Terres and National Audubon Society. 1991), including feathers used in camouflage, migration, overwintering, or courtship (Dunn, et al. 2011). The duration and frequency of juvenile to adult plumage transitions vary among birds, and the transitions occur in response to a mixture of hormonal changes brought about by external stimuli (Podulka, et al. 2004). In contrast, the hatchling (natal down) to juvenile (contour feather) plumage transition happens only once in most birds (the transition starts at posthatch day 7 zebra finch, Figure 19), but the mechanism has never been characterized. By using similar strategies employed in this study, I propose to study the

47

regulatory transition from natal down to contour feathers in altricial zebra finch and precocial chicken to understand the similarities and differences between the two types of birds.

Ultimately, by using feather development as the model, I want to understand how changes in gene regulation affect development and cell differentiation to produce new phenotypes.

48

Orders	Species	DM
Piciformes	*Picoides pubescens*	A
Coraciiformes	*Merops nubicus*	A
Bucerotiformes	*Buceros rhinoceros silvestris*	A
Trogoniformes	*Apaloderma vittatum*	A
Coraciiformes	*Leptosomus discolor*	A
Coliiformes	*Colius striatus*	A
Strigiformes	*Tyto alba*	A
Cathartiformes	*Cathartes aura*	SA
Accipitriformes	*Haliaeetus albicilla*	SA
Accipitriformes	*Haliaeetus leucocephalus*	SA
Cariamiformes	*Cariama cristata*	SP
Falconiformes	*Falco peregrinus*	SA
Psittaciformes	*Melopsittacus undulatus*	A
Psittaciformes	*Nestor notabilis*	A
Passeriformes	*Acanthisitta chloris*	A
Passeriformes	*Manacus vitellinus*	A
Passeriformes	*Corvus brachyrhynchos*	A
Passeriformes	*Taeniopygia guttata*	A
Passeriformes	*Geospiza fortis*	A
Phaethontiformes	*Phaethon lepturus*	A
Eurypygiformes	*Eurypyga helias*	P
Gaviiformes	*Gavia stellata*	SP
Sphenisciformes	*Aptenodytes forsteri*	SP
Sphenisciformes	*Pygoscelis adeliae*	SP
Procellariiformes	*Fulmarus glacialis*	SP
Suliformes	*Phalacrocorax carbo*	A
Pelecaniformes	*Nipponia nippon*	A
Pelecaniformes	*Egretta garzetta*	A
Pelecaniformes	*Pelecanus crispus*	A
Opisthocomiformes	*Opisthocomus hoazin*	A
Gruiformes	*Balearica regulorum gibbericeps*	P/SP
Charadriiformes	*Charadrius vociferus*	P/SP
Musophagiformes	*Tauraco erythrolophus*	A
Otidiformes	*Chlamydotis macqueenii*	P
Cuculiformes	*Cuculus canorus*	A
Caprimulgiformes	*Antrostomus carolinensis*	SP/A
Apodiformes	*Calypte anna*	A
Apodiformes	*Chaetura pelagica*	A
Phoenicopteriformes	*Phoenicopterus ruber ruber*	A
Podicipediformes	*Podiceps cristatus*	SP/A
Columbiformes	*Columba livia*	A
Pteroclidiformes	*Pterocles gutturalis*	SP/A
Mesitornithiformes	*Mesitornis unicolor*	A
Anseriformes	*Anas platyrhynchos domestica*	P
Galliformes	*Meleagris gallopavo*	P
Galliformes	*Gallus gallus*	P
Tinamiformes	*Tinamus guttatus*	P
Struthioniformes	*Camelus australis*	P

Figure 17. Phylogenetic distribution of developmental modes among bird orders.

DM: developmental mode; A: altricial; SA: semialtricial; P: precocial; SP: semiprecocial. Modified from previous studies (Starck and Ricklefs 1998; Podulka, et al. 2004; Zhang, et al. 2014).

49

Figure 18. The juvenile (contour) feather is growing and carries the old natal down on its tip. (Podulka, et al. 2004).
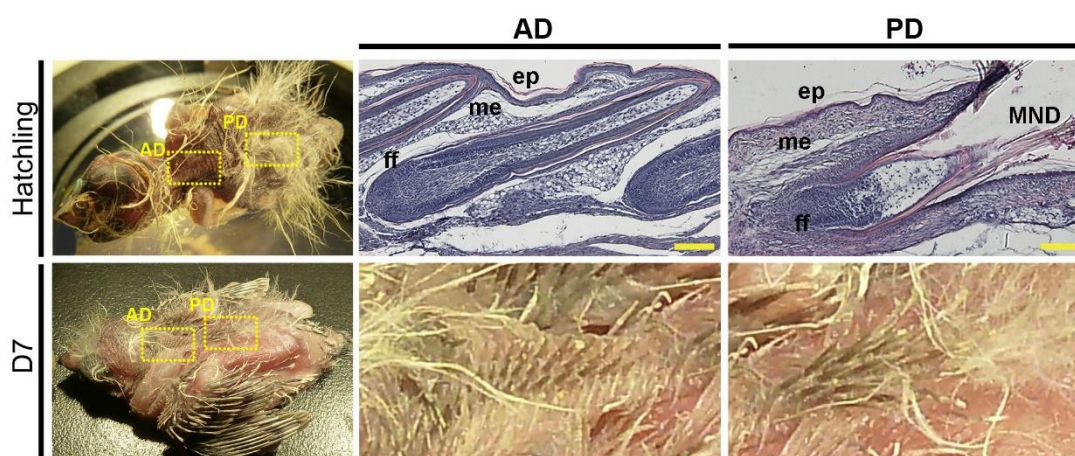
Figure 19. The plumages in hatchling and posthatch day 7 zebra finch. The sections of the hatchling were stained with H&E. AD: anterior dorsal; PD: posterior dorsal; D7: posthatch day 7. ep: epithelium; me: mesenchyme; ff: feather follicle; MND: mature natal down; Scale bar: 100 μm.

REFERENCES

Abzhanov A, Protas M, Grant BR, Grant PR, Tabin CJ. 2004. Bmp4 and morphological variation of beaks in Darwin's finches. Science 305:1462-1465.

Adkins-Regan E. 2009. Hormones and sexual differentiation of avian social behavior. Dev Neurosci 31:342-350.

Alev C, Shinmyozu K, McIntyre BA, Sheng G. 2009. Genomic organization of zebra finch alpha and beta globin genes and their expression in primitive and definitive blood in comparison with globins in chicken. Dev Genes Evol 219:353-360.

Basu M, Mukhopadhyay S, Chatterjee U, Roy SS. 2014. FGF16 promotes invasive behavior of SKOV-3 ovarian cancer cells through activation of mitogen-activated protein kinase (MAPK) signaling pathway. J Biol Chem 289:1415-1428.
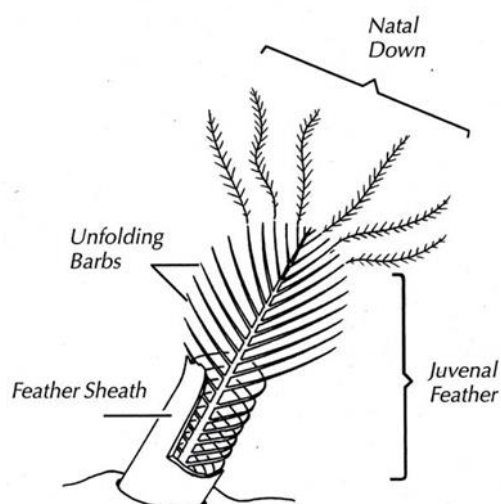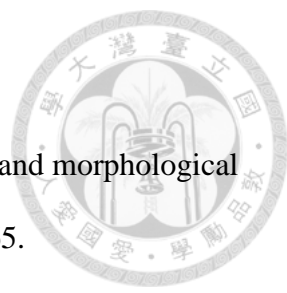
Bhattacharjee MJ, Yu CP, Lin JJ, Ng CS, Wang TY, Lin HH, Li WH. 2016. Regulatory Divergence among Beta-Keratin Genes during Bird Evolution. Mol Biol Evol.

Bicudo JEPW. 2010. Ecological and environmental physiology of birds. Oxford ; New York: Oxford University Press.

Bolger AM, Lohse M, Usadel B. 2014. Trimmomatic: a flexible trimmer for Illumina sequence data. Bioinformatics 30:2114-2120.

Brown WRA, Hubbard SJ, Tickle C, Wilson SA. 2003. The chicken as a model for large-scale analysis of vertebrate gene function. Nature Reviews Genetics 4:87-98.

Charvet CJ, Striedter GF. 2011. Developmental Modes and Developmental Mechanisms can Channel Brain Evolution. Front Neuroanat 5:4.

Chen CF, Foley J, Tang PC, Li A, Jiang TX, Wu P, Widelitz RB, Chuong CM. 2015. Development, regeneration, and evolution of feathers. Annu Rev Anim Biosci

3:169-195.

Chen CK, Ng CS, Wu SM, Chen JJ, Cheng PL, Wu P, Lu MJ, Chen DR, Chuong CM,
Cheng HC, et al. 2016. Regulatory Differences in Natal Down Development
between Altricial Zebra Finch and Precocial Chicken. Mol Biol Evol.

Chuong C-M. 1998. Molecular basis of epithelial appendage morphogenesis. Austin, TX:
R.G. Landes.

Chuong CM, Widelitz RB, Ting-Berreth S, Jiang TX. 1996. Early events during avian
skin appendage regeneration: dependence on epithelial-mesenchymal interaction
and order of molecular reappearance. J Invest Dermatol 107:639-646.

Clayton DF, Balakrishnan CN, London SE. 2009. Integrating genomes, brain and
behavior in the study of songbirds. Curr Biol 19:R865-873.

Clayton DF, George JM, Mello CV, Siepka SM. 2009. Conservation and expression of
IQ-domain-containing calpacitin gene products (neuromodulin/GAP-43,
neurogranin/RC3) in the adult and developing oscine song control system. Dev
Neurobiol 69:124-140.

Consortium ICGS. 2004. Sequence and comparative analysis of the chicken genome
provide unique perspectives on vertebrate evolution. Nature 432:695-716.

Daly TJ, Buffenstein R. 1998. Skin morphology and its role in thermoregulation in
mole-rats, Heterocephalus glaber and Cryptomys hottentotus. J Anat 193 (Pt
4):495-502.

Deeming DC, Reynolds SJ. 2015. Nests, eggs, and incubation : new ideas about avian
reproduction. In.

Dhouailly D. 2009. A new scenario for the evolutionary origin of hair, feather, and avian
scales. J Anat 214:587-606.
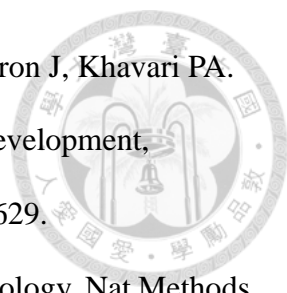
Dial KP, Jackson BE, Segre P. 2008. A fundamental avian wing-stroke provides a new perspective on the evolution of flight. Nature 451:985-989.

Dunn JL, Alderfer JK, National Geographic Society (U.S.). 2011. National Geographic field guide to the birds of North America. Washington, D.C.: National Geographic Society.

Ewing B, Green P. 1998. Base-calling of automated sequencer traces using phred. II. Error probabilities. Genome Res 8:186-194.

Geiss GK, Bumgarner RE, Birditt B, Dahl T, Dowidar N, Dunaway DL, Fell HP, Ferree S, George RD, Grogan T, et al. 2008. Direct multiplexed measurement of gene expression with color-coded probe pairs. Nat Biotechnol 26:317-325.

Greenwold MJ, Sawyer RH. 2010. Genomic organization and molecular phylogenies of the beta (beta) keratin multigene family in the chicken (Gallus gallus) and zebra finch (Taeniopygia guttata): implications for feather evolution. BMC Evol Biol 10:148.

Hamburger V, Hamilton HL. 1992a. A Series of Normal Stages in the Development of the Chick-Embryo, (Reprinted from Journal of Morphology, Vol 88, 1951). Developmental Dynamics 195:231-&.

Hamburger V, Hamilton HL. 1992b. A series of normal stages in the development of the chick embryo. 1951. Dev Dyn 195:231-272.

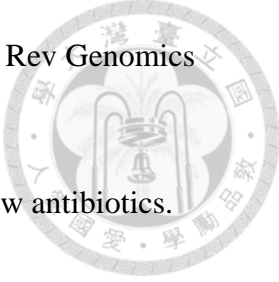Hornik C, Krishan K, Yusuf F, Scaal M, Brand-Saberi B. 2005. cDermo-1 misexpression induces dense dermis, feathers, and scales. Dev Biol 277:42-50.

Hughes SH. 2004. The RCAS vector system. Folia Biologica 50:107-119.

Jung HS, Francis-West PH, Widelitz RB, Jiang TX, Ting-Berreth S, Tickle C, Wolpert L, Chuong CM. 1998. Local inhibitory action of BMPs and their relationships with

activators in feather formation: implications for periodic patterning. Dev Biol 196:11-23.

Lande R. 1978. Evolutionary Mechanisms of Limb Loss in Tetrapods. Evolution 32:73-92.

Langmead B, Trapnell C, Pop M, Salzberg SL. 2009. Ultrafast and memory-efficient alignment of short DNA sequences to the human genome. Genome Biol 10:R25.

Laurell T, Nilsson D, Hofmeister W, Lindstrand A, Ahituv N, Vandermeer J, Amilon A, Anneren G, Arner M, Pettersson M, et al. 2014. Identification of three novel FGF16 mutations in X-linked recessive fusion of the fourth and fifth metacarpals and possible correlation with heart disease. Mol Genet Genomic Med 2:402-411.

Lin CM, Jiang TX, Baker RE, Maini PK, Widelitz RB, Chuong CM. 2009. Spots and stripes: pleomorphic patterning of stem cells via p-ERK-dependent cell chemotaxis shown by feather morphogenesis and mathematical simulation. Dev Biol 334:369-382.

Liu WY, Chang YM, Chen SC, Lu CH, Wu YH, Lu MY, Chen DR, Shih AC, Sheue CR, Huang HC, et al. 2013. Anatomical and transcriptional dynamics of maize embryonic leaves during seed germination. Proc Natl Acad Sci U S A 110:3979-3984.

Loftus SK, Larson DM, Watkins-Chow D, Church DM, Pavan WJ. 2001. Generation of RCAS vectors useful for functional genomic analyses. DNA Res 8:221-226.

Mandler M, Neubuser A. 2004. FGF signaling is required for initiation of feather placode development. Development 131:3333-3343.

Mardis ER. 2008a. The impact of next-generation sequencing technology on genetics. Trends Genet 24:133-141.

Mardis ER. 2008b. Next-generation DNA sequencing methods. Annu Rev Genomics Hum Genet 9:387-402.

McDevitt D, Rosenberg M. 2001. Exploiting genomics to discover new antibiotics. Trends Microbiol 9:611-617.

McKinnell IW, Turmaine M, Patel K. 2004. Sonic Hedgehog functions by localizing the region of proliferation in early developing feather buds. Dev Biol 272:76-88.

Meinhardt H, Gierer A. 2000. Pattern formation by local self-activation and lateral inhibition. BioEssays : news and reviews in molecular, cellular and developmental biology 22:753-760.

Metzker ML. 2005. Emerging technologies in DNA sequencing. Genome Res 15:1767-1776.

Mortazavi A, Williams BA, McCue K, Schaeffer L, Wold B. 2008. Mapping and quantifying mammalian transcriptomes by RNA-Seq. Nat Methods 5:621-628.

Mou C, Pitel F, Gourichon D, Vignoles F, Tzika A, Tato P, Yu L, Burt DW, Bed'hom B, Tixier-Boichard M, et al. 2011. Cryptic patterning of avian skin confers a developmental facility for loss of neck feathering. PLoS Biol 9:e1001028.

Murray JR, Varian-Ramos CW, Welch ZS, Saha MS. 2013. Embryological staging of the Zebra Finch, Taeniopygia guttata. J Morphol 274:1090-1110.

Ng CS, Chen CK, Fan WL, Wu P, Wu SM, Chen JJ, Lai YT, Mao CT, Lu MY, Chen DR, et al. 2015. Transcriptomic analyses of regenerating adult feathers in chicken. BMC Genomics 16:756.

Noramly S, Freeman A, Morgan BA. 1999. beta-catenin signaling can initiate feather bud development. Development 126:3509-3521.

Oh HM, Choi SC, Lee HS, Chun CH, Seo GS, Choi EY, Lee HJ, Lee MS, Yeom JJ, Choi

55
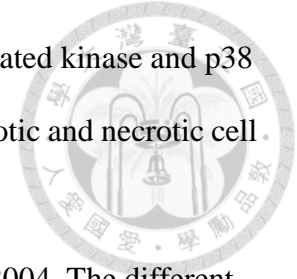
SJ, et al. 2004. Combined action of extracellular signal-regulated kinase and p38 kinase rescues Molt4 T cells from nitric oxide-induced apoptotic and necrotic cell death. Free Radic Biol Med 37:463-479.

Olivera-Martinez I, Viallet JP, Michon F, Pearton DJ, Dhouailly D. 2004. The different steps of skin formation in vertebrates. Int J Dev Biol 48:107-115.

Ornitz DM, Itoh N. 2001. Fibroblast growth factors. Genome Biol 2:REVIEWS3005.

Paznekas WA, Okajima K, Schertzer M, Wood S, Jabs EW. 1999. Genomic organization, expression, and chromosome location of the human SNAIL gene (SNAI1) and a related processed pseudogene (SNAI1P). Genomics 62:42-49.

Pinaud R. 2010. Genome of a songbird unveiled. J Biol 9:19.

Podulka S, Rohrbaugh RW, Bonney R. 2004. Handbook of bird biology. Ithaca, NY: Cornell Lab of Ornithology in association with Princeton University Press.

Protas ME, Trontelj P, Patel NH. 2011. Genetic basis of eye and pigment loss in the cave crustacean, Asellus aquaticus. Proc Natl Acad Sci U S A 108:5702-5707.

Prum RO. 2005. Evolution of the morphological innovations of feathers. J Exp Zool B Mol Dev Evol 304:570-579.

Prum RO, Brush AH. 2002. The evolutionary origin and diversification of feathers. Q Rev Biol 77:261-295.

Reimand J, Arak T, Vilo J. 2011. g:Profiler--a web server for functional interpretation of gene lists (2011 update). Nucleic Acids Res 39:W307-315.

Reimand J, Kull M, Peterson H, Hansen J, Vilo J. 2007. g:Profiler--a web-based toolset for functional profiling of gene lists from large-scale experiments. Nucleic Acids Res 35:W193-200.

Sang H. 2004. Prospects for transgenesis in the chick. Mech Dev 121:1179-1186.

Scholl FA, Dumesic PA, Barragan DI, Harada K, Bissonauth V, Charron J, Khavari PA. 2007. Mek1/2 MAPK kinases are essential for Mammalian development, homeostasis, and Raf-induced hyperplasia. Dev Cell 12:615-629.

Schuster SC. 2008. Next-generation sequencing transforms today's biology. Nat Methods 5:16-18.

Song HK, Lee SH, Goetinck PF. 2004. FGF-2 signaling is sufficient to induce dermal condensations during feather development. Dev Dyn 231:741-749.

Starck JM, Ricklefs RE. 1998. Avian growth and development : evolution within the altricial-precocial spectrum. New York: Oxford University Press.

Stern CD. 2004. The chick embryo--past, present and future as a model system in developmental biology. Mech Dev 121:1011-1013.

Stern CD. 2005. The chick: A great model system becomes even greater. Developmental Cell 8:9-17.

Strasser B, Mlitz V, Hermann M, Tschachler E, Eckhart L. 2015. Convergent evolution of cysteine-rich proteins in feathers and hair. BMC Evol Biol 15:82.

Tao H, Yoshimoto Y, Yoshioka H, Nohno T, Noji S, Ohuchi H. 2002. FGF10 is a mesenchymally derived stimulator for epidermal development in the chick embryonic skin. Mech Dev 116:39-49.

Tarazona S, Garcia-Alcalde F, Dopazo J, Ferrer A, Conesa A. 2011. Differential expression in RNA-seq: a matter of depth. Genome Res 21:2213-2223.

Terres JK, National Audubon Society. 1991. The Audubon Society encyclopedia of North American birds. New York: Wings Books : Distributed by Outlet Book Co.

Trapnell C, Hendrickson DG, Sauvageau M, Goff L, Rinn JL, Pachter L. 2013. Differential analysis of gene regulation at transcript resolution with RNA-seq. Nat

Biotechnol 31:46-53.

Trapnell C, Pachter L, Salzberg SL. 2009. TopHat: discovering splice junctions with RNA-Seq. Bioinformatics 25:1105-1111.

Vleck CM, Vleck D. 1987. Metabolism and energetics of avian embryos. J Exp Zool Suppl 1:111-125.

Warnes GR, Bolker B, Bonebakker L, Gentleman R, Huber W, Liaw A, Lumley T, Maechler M, Magnusson A, Moeller S. 2009. gplots: Various R programming tools for plotting data. R package version 2.

Warren WC, Clayton DF, Ellegren H, Arnold AP, Hillier LW, Kunstner A, Searle S, White S, Vilella AJ, Fairley S, et al. 2010. The genome of a songbird. Nature 464:757-762.

Wells KL, Hadad Y, Ben-Avraham D, Hillel J, Cahaner A, Headon DJ. 2012. Genome-wide SNP scan of pooled DNA reveals nonsense mutation in FGF20 in the scaleless line of featherless chickens. BMC Genomics 13:257.

Widelitz RB, Jiang TX, Lu J, Chuong CM. 2000. beta-catenin in epithelial morphogenesis: conversion of part of avian foot scales into feather buds with a mutated beta-catenin. Dev Biol 219:98-114.

Widelitz RB, Jiang TX, Noveen A, Chen CW, Chuong CM. 1996. FGF induces new feather buds from developing avian skin. J Invest Dermatol 107:797-803.

Wright MT. 2006. Birds of the world : recommended English names. London: Christopher Helm.

Yue Z, Jiang TX, Wu P, Widelitz RB, Chuong CM. 2012. Sprouty/FGF signaling regulates the proximal-distal feather morphology and the size of dermal papillae. Dev Biol 372:45-54.

Zann RA. 1996. The zebra finch : a synthesis of field and laboratory studies. Oxford ; New York: Oxford University Press.

Zhang GJ, Li C, Li QY, Li B, Larkin DM, Lee C, Storz JF, Antunes A, Greenwold MJ, Meredith RW, et al. 2014. Comparative genomics reveals insights into avian genome evolution and adaptation. Science 346:1311-1320.

Zheng X, Zhou Z, Wang X, Zhang F, Zhang X, Wang Y, Wei G, Wang S, Xu X. 2013. Hind wings in Basal birds and the evolution of leg feathers. Science 339:1309-1312.

Zhou Z, Zhang F. 2004. A precocial avian embryo from the Lower Cretaceous of China. Science 306:653.

APPENDIX

Appendix Figures
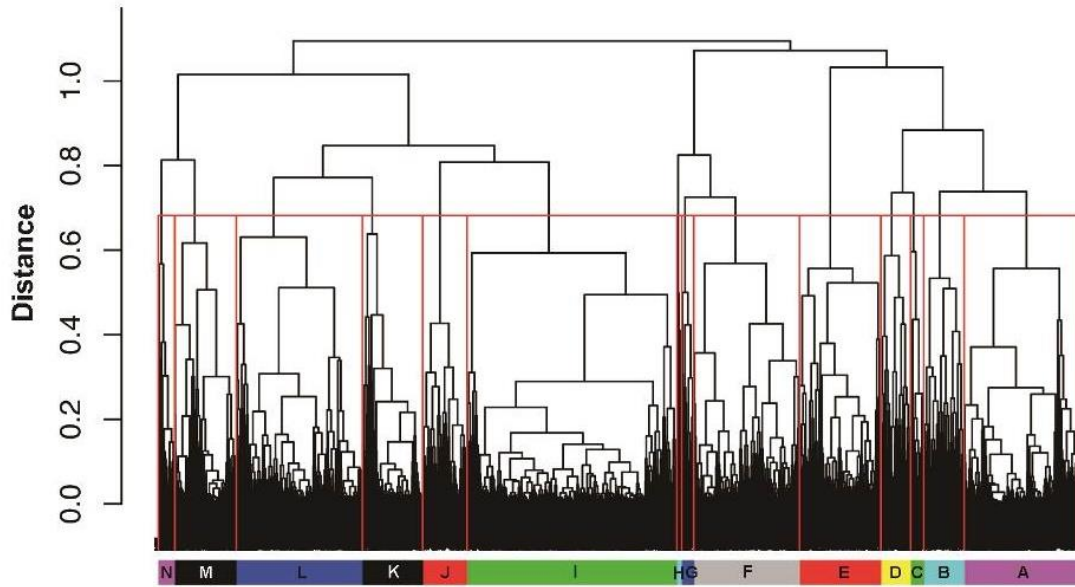
Figure A1. The cluster dendrogram of differential expressed genes. The cut-off for

Cluster A-N was set to be 0.65 as indicated by the red line.
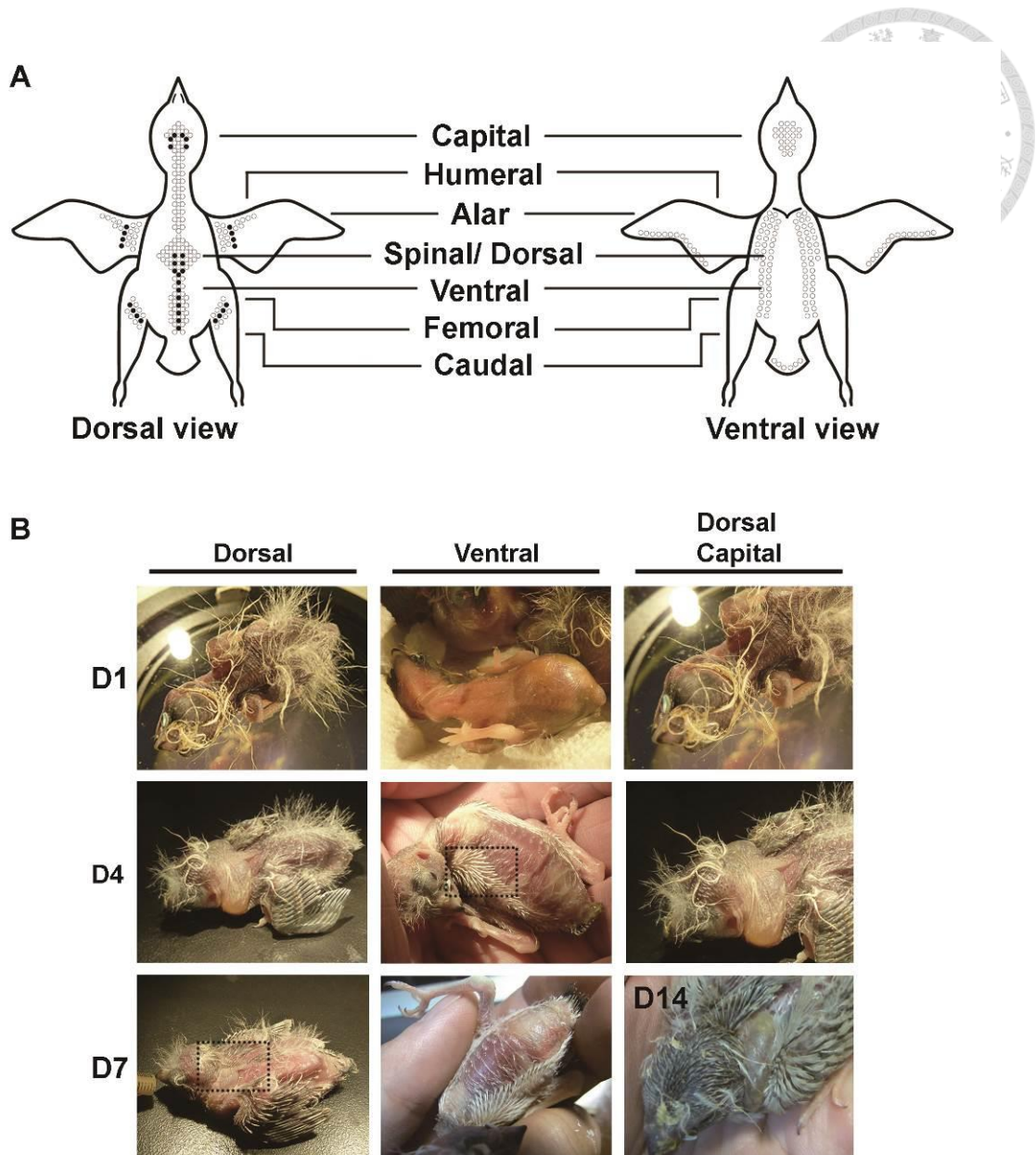
Figure A2. Type I and Type II feather formations in body regions of zebra finch. (A) The distributions of feather tracts and two types of feather formations. Open circles: Type I feather buds in anterior dorsal skin, part of the capital skin, and ventral skin. Black circles: Type II feather buds in posterior dorsal skin and part of the capital skin. (B) Growth of contour feathers in the Type I feather buds. The square with dotted lines shows the contour feathers formed in Type I region (anterior dorsal skin in D7 and ventral skin in D4).
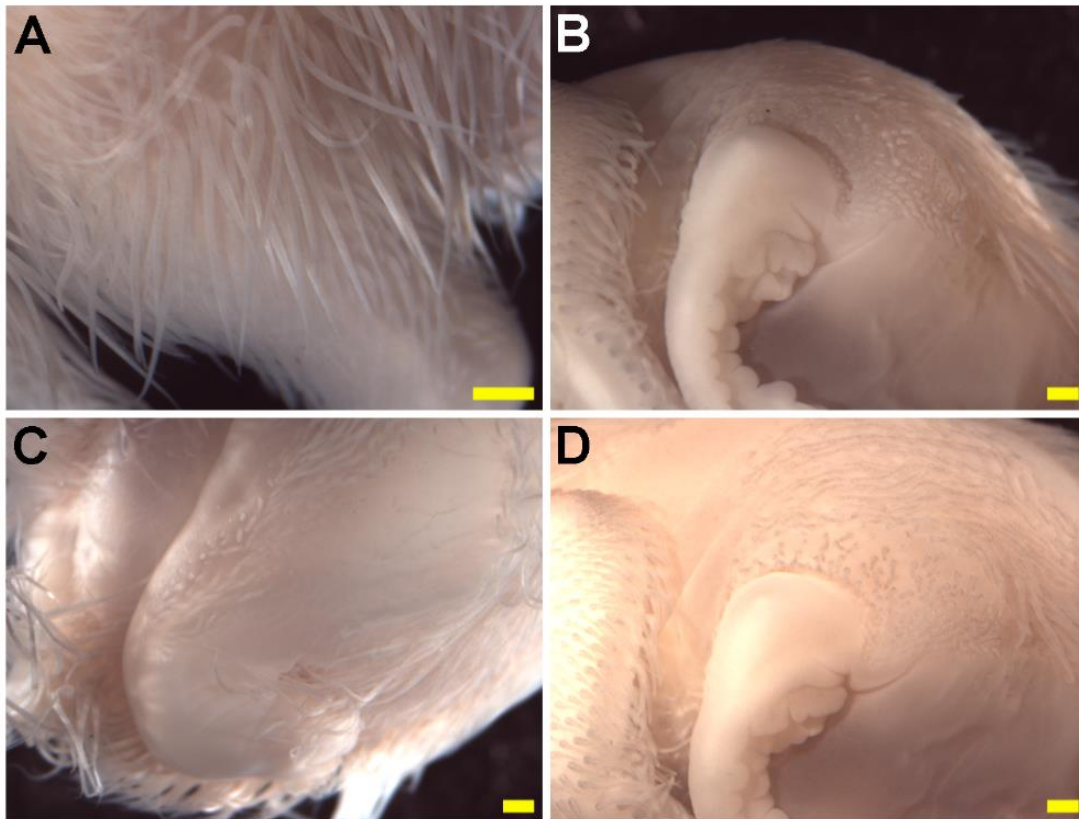
Figure A3. The phenotypes of FGF16 overexpression in different individuals of E12 chicken. (A) The control leg without RCAS-FGF16 microinjection. (B-D) Three individuals of RCAS-FGF16 microinjections. Scale bar: 1 mm.
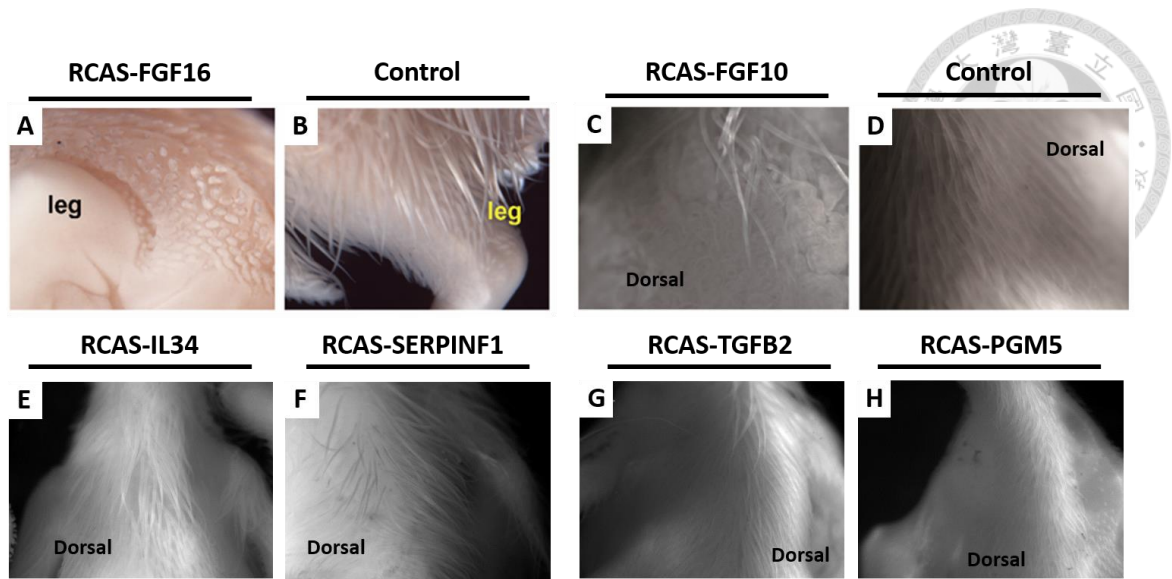
Figure A4. All the genes overexpressed in chicken by RCAS virus system. Six genes were constructed in RCAS virus and microinjected into E3 chicken then observed the phenotypes in E12 chicken, but only overexpressed FGF16 and FGF10 showed suppressed feather buds (A-D). (E) IL34: Interleukin 34. (F) SERPINF1: Serpin F1. (G) TGFB2: Transforming growth factor beta 2. (H) Phosphoglucomutase 5.

Appendix Tables

Table A1. Primer pair sequences used in Quantitative PCR.

Gene name	Forward (F) or Reverse (R)	Sequence (5'-3')
ACTA1	F	TCACCATCGGCAATGAGCGT
	R	TGTCTCATGGATCCCAGCGGA
ACTC1	F	AATGGCCACAGCTGCTTCGT
	R	ATAAGGTTTCCGGGCAGCGG
BMP4	F	CCGCCACGCTCTCTATGTGG
	R	GGCGTGGTTGGTGGAGTTGA
BMP7	F	CCAGAGACTGTGCCGAAACC
	R	TTTTAAGATAACGTTGGAGCTGT
CDH1	F	CGCTCAGGGTCTGGGATGGC
	R	CACGTCGTTGGTCTGCGGGA
CDH2	F	AAAGCAGCCGACAACGACCCT
	R	ATCCAGCAGTGGAGCCGCTT
CHRNA1	F	TGGAGAATCACCGCGATGCC
	R	GCTGCTTCAGGCGCACATTG
FGF10	F	TGGTGCCTCAGCCTTTTCCCA
	R	GCCGAGGTCATGGCAGGTGA
FGF16	F	CCCGTGAGGGGTACAGGACT
	R	ATGGCAGGGATTTTGGCAGGG

Table A1 continue

Gene name	Forward (F) or Reverse (R)	Sequence (5'-3')
FGF20	F	GCCAAGACCACAGCCTCTT
	R	TTCCAAGGTAAAGGCCACTG
FGFR1	F	CTCGGTGTTCTCCCACGACC
	R	GAGCCTCAGTGCCGCTTCAG
FGFR4	F	CACCGACAAGGACCTGGCTG
	R	GGTTGCCCTTGGCAGCAAAC
HOXA2	F	CCATCGCTTGCTGAGTGCCT
	R	GGTTCAGGCTGGGGATGGTC
HOXC6	F	GAGGCGGATCGAAATCGCCA
	R	CCCGGAGAGGGTCGAGCTTA
MYOD	F	AAGACCACCAACGCTGACCG
	R	GATCTCCACCTTGGGCAGGC
MYOG	F	GCGCAAAACCGTGTCCATCG
	R	GCAGGATCTCCACCTTGGGC
NCAM	F	GGACCCGGCCCGAGAAACAA
	R	GCACACGTACTCTCCGGCGT
PTCH1	F	GCCTTGAGCCACCCTGTACG
	R	GGCTGAGCCCAAGTAAGCCC
SNAI1	F	GCAACCGGGCCTTTGCTGAC
	R	TGCAGCAGCGACATACGGGA

Table A1 continue

Gene name	Forward (F) or Reverse (R)	Sequence (5'-3')
TBP	F	CACAGCAAGCGACACAGGGA
	R	AGGTGTGGTTCCCGGCAAAG
TGFB2	F	TGAGTCGCAACAGCCCAGTC
	R	AAGTGGACGCAGGCAGCAAT
TNC	F	AGCAAGTGGGGACGCAGACC
	R	GGCGGGGAATGTTGATGCGG
TNNC1	F	AAGCCAGATGGACAGCCCGA
	R	ACCCTTCTCAGCGCTCAGTCT
TWIST2	F	CGTGGCTCACGAGAGGCTGAG
	R	CGGCGGTGGCTAGTGTGAGG

66
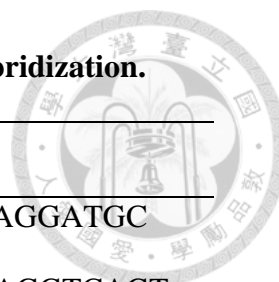
Table A2. Primer pair sequences used in whole mount *in situ* hybridization.

Gene name	Forward (F) or Reverse (R)	Sequence (5'-3')
CTNNB1	F	GGCGGATACGGTCAGGATGC
	R	TCCAAAGCAAGCAAGGTCAGT
SHH	F	CTGGTGAAGGACCTGAGCCCT
	R	GCCCAACTGTGCTCCTCGAT
SNAI1	F	TGGCGCTTGGCAGTACGATG
	R	GGCAGCACGGAGGGAACTAA
TWIST2	F	CAAGGGGGAGCTGGTTCTCG
	R	CTGCTAGTGGGATGCGGACA

Table A3. Primer pair sequences used in RCAS experiments.

Gene name	Forward (F) or Reverse (R)	Sequence (5'-3')
FGF16	F	ATGGCCGAGGTGGGCG
	R	TCACCTGTAGTGGAAGAGGTC
FGF10	F	TCCAACGCCCAGAGTTTCAG
	R	GAGCCTTTGGTTCAACTGCAT

Table A4. Information of the expressed genes. The table with FPKM value, DEGs, and clusters of all the expressed genes is in the following link:

http://mbe.oxfordjournals.org/content/early/2016/04/26/molbev.msw085/suppl/DC1

67

Table A5. The top 10 enriched GO categories of cluster A.

p-value	T	Q	Q&T	term ID	term type	term name
1.93E-28	108	1413	59	GO:0005882	CC	intermediate filament
4.28E-26	98	1413	54	GO:0005200	MF	structural constituent of cytoskeleton
1.77E-21	145	1413	61	GO:0045111	CC	intermediate filament cytoskeleton
9.77E-16	24	1412	21	HP:0002202	hp	Pleural effusion
1.24E-13	18	1412	17	HP:0040130	hp	Abnormal serum iron
1.24E-13	18	1412	17	HP:0003452	hp	Increased serum iron
3.65E-12	22	1412	18	HP:0000802	hp	Impotence
5.71E-11	21	1413	17	GO:0042612	CC	MHC class I protein complex
2.29E-10	22	1413	17	GO:0042605	MF	peptide antigen binding
4.31E-10	23	1412	17	HP:0000029	hp	Testicular atrophy

Note: T: Total number of genes associated to functional term; Q: number of genes in input list; Q&T: number of genes in the list associated to functional term; CC: cellular component; MF: molecular function; hp: human phenotype.

68

Table A6. The top 10 enriched GO categories of cluster B.

p-value	T	Q	Q&T	term ID	term type	term name
5.46E-07	11	501	8	GO:0034141	BP	positive regulation of toll-like receptor 3 signaling pathway
1.59E-06	12	501	8	GO:0045918	BP	negative regulation of cytolysis
1.59E-06	12	501	8	GO:0034139	BP	regulation of toll-like receptor 3 signaling pathway
4.01E-06	13	501	8	GO:0042268	BP	regulation of cytolysis
6.56E-05	30	501	10	GO:0034121	BP	regulation of toll-like receptor signaling pathway
1.03-04	6087	501	263	GO:0005737	CC	cytoplasm
1.17-04	18	501	8	GO:0034123	BP	positive regulation of toll-like receptor signaling pathway
1.52-04	25	501	9	GO:0019835	BP	cytolysis
6.05-04	36	495	9	KEGG:04623	KEGG	Cytosolic DNA-sensing pathway
3.69-03	4219	501	190	GO:0044444	CC	cytoplasmic part

Note: T: Total number of genes associated to functional term; Q: number of genes in input list; Q&T: number of genes in the list associated to functional term; CC: cellular component; MF: molecular function; hp: human phenotype.

Table A7. The top 10 enriched GO categories from cluster F.

p-value	T	Q	Q&T	term ID	term type	term name
5.27E-30	2420	1384	401	GO:0044428	CC	nuclear part
7.71E-30	1066	1384	227	GO:0003723	MF	RNA binding
8.65E-28	7873	1384	947	GO:0043226	CC	organelle
3.12E-27	2135	1384	359	GO:0031981	CC	nuclear lumen
3.21E-27	2420	1384	393	GO:0003676	MF	nucleic acid binding
1.71E-26	831	1384	186	GO:0044822	MF	poly(A) RNA binding
3.24E-26	7053	1384	868	GO:0043229	CC	intracellular organelle
8.85E-25	4426	1384	606	GO:0044446	CC	intracellular organelle part
6.56E-24	3596	1384	515	GO:0034641	BP	cellular nitrogen compound metabolic process
1.8E-23	4548	1384	614	GO:0044422	CC	organelle part

Note: T: Total number of genes associated to functional term; Q: number of genes in input list; Q&T: number of genes in the list associated to functional term; CC: cellular component; MF: molecular function; hp: human phenotype.
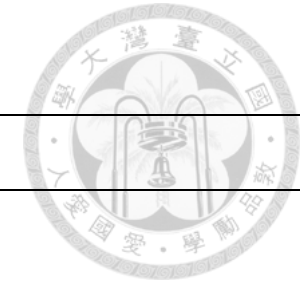
Table A8. The top 10 enriched GO categories from cluster J.

p-value	T	Q	Q&T	term ID	term type	term name
7.33E-15	126	546	32	GO:0030016	CC	myofibril
2.56E-14	131	546	32	GO:0043292	CC	contractile fiber
3.13E-12	115	546	28	GO:0044449	CC	contractile fiber part
3.85E-12	107	546	27	GO:0030017	CC	sarcomere
3.43E-07	102	546	21	GO:0055002	BP	striated muscle cell development
4.87E-07	75	546	18	GO:0031674	CC	I band
3.51E-06	115	546	21	GO:0055001	BP	muscle cell development
4.17E-06	66	546	16	GO:0030018	CC	Z disc
1.35E-05	45	546	13	GO:0030239	BP	myofibril assembly
2.96E-05	153	546	23	GO:0006936	BP	muscle contraction

Note: T: Total number of genes associated to functional term; Q: number of genes in input list; Q&T: number of genes in the list associated to functional term; CC: cellular component; MF: molecular function; hp: human phenotype.

71

Table A9. The top 10 enriched GO categories from cluster L.

p-value	T	Q	Q&T	term ID	term type	term name
4.21E-12	2794	1575	418	GO:0007275	BP	multicellular organismal development
1.02E-11	1723	1575	283	GO:0009653	BP	anatomical structure morphogenesis
1.41E-11	3368	1575	484	GO:0044767	BP	single-organism developmental process
3.35E-11	3392	1575	485	GO:0032502	BP	developmental process
3.4E-09	3078	1575	438	GO:0048856	BP	anatomical structure development
1.1E-08	2571	1575	375	GO:0048731	BP	system development
2.43E-08	600	1575	119	GO:0022603	BP	regulation of anatomical structure morphogenesis
3.29E-08	1359	1575	222	GO:0050793	BP	regulation of developmental process
1.98E-07	3668	1575	497	GO:0044707	BP	single-multicellular organism process
2.07E-07	1033	1575	176	GO:2000026	BP	regulation of multicellular organismal development

Note: T: Total number of genes associated to functional term; Q: number of genes in input list; Q&T: number of genes in the list associated to functional term; CC: cellular component; MF: molecular function; hp: human phenotype.

72

Table A10. The top 10 enriched GO categories from cluster M.

p-value	T	Q	Q&T	term ID	term type	term name
2E-12	736	753	94	GO:0005783	CC	endoplasmic reticulum
2E-10	1926	753	175	GO:0012505	CC	endomembrane system
2E-08	368	753	54	GO:0044432	CC	endoplasmic reticulum part
2E-07	909	753	95	GO:0098588	CC	bounding membrane of organelle
2E-07	133	748	27	KEGG:04141	KEGG	Protein processing in endoplasmic reticulum
4E-06	1290	753	118	GO:0031090	CC	organelle membrane
5E-05	323	753	43	GO:0042175	CC	nuclear outer membrane-endoplasmic reticulum membrane network
7E-05	291	753	40	GO:0031012	CC	extracellular matrix
8E-05	316	753	42	GO:0005789	CC	endoplasmic reticulum membrane
9E-05	38	753	13	GO:0005793	CC	endoplasmic reticulum-Golgi intermediate compartment

Note: T: Total number of genes associated to functional term; Q: number of genes in input list; Q&T: number of genes in the list associated to functional term; CC: cellular component; MF: molecular function; hp: human phenotype.
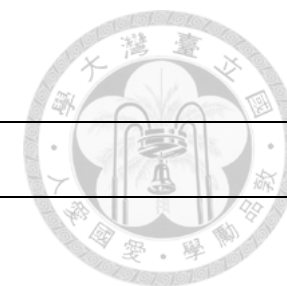
Table A11. The top 10 enriched GO categories from cluster N.

p-value	T	Q	Q&T	term ID	term type	term name
1.29E-03	115	207	11	GO:0044449	CC	contractile fiber part
3.21E-03	126	207	11	GO:0030016	CC	myofibril
3.95E-03	245	207	15	GO:0042692	BP	muscle cell differentiation
4.71E-03	131	207	11	GO:0043292	CC	contractile fiber
4.78E-03	44	207	7	GO:0060415	BP	muscle tissue morphogenesis
6.17E-03	254	207	15	GO:0060537	BP	muscle tissue development
1.39E-02	238	207	14	GO:0014706	BP	striated muscle tissue development
1.57E-02	51	203	5	KEGG:04260	ke	Cardiac muscle contraction
1.68E-02	184	203	9	KEGG:04010	ke	MAPK signaling pathway
3.80E-02	165	203	8	KEGG:04810	ke	Regulation of actin cytoskeleton

Note: T: Total number of genes associated to functional term; Q: number of genes in input list; Q&T: number of genes in the list associated to functional term; CC: cellular component; MF: molecular function; hp: human phenotype.

74

CURRICULUM VITAE

Chih-Kuan Chen (1/2017)

Ph. D. student

Institute of Ecology and Evolutionary Biology, National Taiwan University, Taiwan.

Biodiversity Research Center, Academia Sinica, Taiwan.

Education and Work Experience:

2009.09~2017.01   Ph. D. Institute of Ecology and Evolutionary Biology, National

Taiwan University, Taipei

2008.03~2009.08   Research assistant. Academia Sinica NGS core facility

2007.03~2008.02   Alternative military service. Ministry of Justice Investigation

Bureau

2007.01   M.S. Institute of Plant Biology, National Taiwan University, Taipei

2004.06   B.S. Department of Biological Resource, Chia-Yi University, Chia-Yi

Publications:

First author in Ph.D. Program

Chen CK, Ng CS, Wu SM, Chen JJ, Cheng PL, Wu P, Lu MY, Chen DR, Chuong CM,

Cheng HC*, Ting CT*, Li WH*, 2016, "Regulatory Differences in Natal

Down Development between Altricial Zebra Finch and Precocial Chicken.",

Molecular biology and evolution, 33(8), 2030-43.

Chih-Kuan Chen, Chun-Ping Yu, Sung-Chou Li, Siao-Man Wu, Mei-Yeh Jade Lu,

Di-Rong Chen, Chen Siang Ng*, Chau-Ti Ting*, Wen-Hsiung Li*, 2016,

"Identification and evolutionary analysis of long non-coding RNAs in birds.",

BMC Genomics, in press.
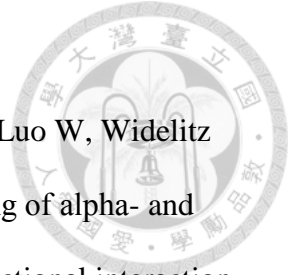
Co-author in Ph.D. Program

Wu P, Ng CS, Yan J, Lai YC, **Chen CK**, Lai YT, Wu SM, Chen JJ, Luo W, Widelitz RB, Li WH*, Chuong CM*, 2015, "Topographical mapping of alpha- and beta-keratins on developing chicken skin integuments: Functional interaction and evolutionary perspectives.", *Proceedings of the National Academy of Sciences of the United States of America*, 112(49), E6770-E6779.

Chen Siang Ng, **Chih-Kuan Chen**, Wen-Lang Fan, Ping Wu, Siao-Man Wu, Jiun-Jie Chen, Yu-Ting Lai, Chi-Tang Mao, Mei-Yeh Jade Lu, Di-Rong Chen, Ze-Shiang Lin, Kai-Jung Yang, Yuan-An Sha, Tsung-Che Tu, Chih-Feng Chen, Cheng-Ming Chuong and Wen-Hsiung Li*, 2015, "Transcriptomic analyses of regenerating adult feathers in chicken", *BMC Genomics*, 16, 756.

Ng CS, Wu P, Fan WL, Yan J, **Chen CK**, Lai YT, Wu SM, Mao CT, Chen JJ, Lu MY, Ho MR, Widelitz RB, Chen CF, Chuong CM, Li WH*, 2014, "Genomic Organization, Transcriptomic Analysis, and Functional Characterization of Avian alpha- and beta-Keratins in Diverse Feather Forms.", *Genome biology and evolution*, 6(9), 2258-73.

Fan WL, Ng CS, Chen CF, Lu MY, Chen YH, Liu CJ, Wu SM, **Chen CK**, Chen JJ, Mao CT, Lai YT, Lo WS, Chang WH, Li WH*, 2013, "Genome-wide patterns of genetic variation in two domestic chickens", *Genome biology and evolution*, 5, 1376-1392.

Co-author during research assistant

Wang TY, Chen HL, Lu MY, Chen YC, Sung HM, Mao CT, Cho HY, Ke HM, Hwa TY, Ruan SK, Hung KY, **Chen CK,** Li JY, Wu YC, Chen YH, Chou SP, Tsai YW, Chu TC, Shih CC, Li WH*, Shih MC, 2011, "Functional

76

doi:10.6342/NTU201700010

characterization of cellulases identified from the cow rumen fungus

Neocallimastix patriciarum W5 by transcriptomic and secretomic analyses.",

Biotechnology for biofuels, 4, 24.
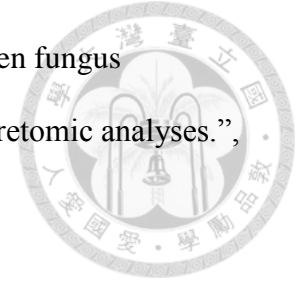
Academic Honors:

2016.09   Exchange student travel award, Genetic Society of Japan (GSJ), Japan

2016.06   The best Ph.D. student poster award, 2016 NTU & NTNU Joint Symposium

on Ecology and Evolutionary Biology

2014.07   Semi-Finalist for best student oral presentation, Taiwan Society of

Evolution and Computational Biology

77